



Stable isotopes of pedogenic carbonates as indicators of paleoecology in the Plio-Pleistocene (upper Bed I), western margin of the Olduvai Basin, Tanzania

Nancy E. Sikes^{a,b,*}, Gail M. Ashley^c

^a Human Origins Program, National Museum of Natural History, Smithsonian Institution, Washington, DC 20560, USA

^b SWCA[®] Environmental Consultants, 3840 Rosin Court, Suite 130, Sacramento, CA 95834, USA

^c Department of Geological Sciences, Rutgers University, 610 Taylor Road, Piscataway, NJ 08854, USA

Received 4 November 2005; accepted 1 December 2006

Abstract

Paleosol carbonates from trenches excavated as part of a landscape-scale project in Bed I of Olduvai Gorge, Tanzania, were analyzed for stable carbon and oxygen isotopic composition. The ~60,000-year interval (~1.845–1.785 Ma) above Tuff IB records evidence for lake and fluvial sequences, volcanic eruptions, eolian and pedogenic processes, and the development of a fluvial plain in the western margin of the basin. Significant temporal variation in the carbonate $\delta^{18}\text{O}$ values records variation of local precipitation and supports the shifts in climatic conditions interpreted from the lithologic record. During this period, carbonate $\delta^{13}\text{C}$ values varied between depositional facies indicating that the paleolandscape supported a local biomass of about 40–60% C_4 plants within a mosaic of grassy woodlands and wooded grasslands. The lithologic and stable isotope record in this small lake basin indicates the area was much wetter, with more woody C_3 plants, during this interval than is the semi-arid area today. The record also reflects the variation in climatic conditions (wet/dry) documented by other global climate proxies for this time.

© 2007 Elsevier Ltd. All rights reserved.

Keywords: Paleoclimate; Paleosols; Olduvai Gorge; Paleolandscape; Early hominins

Introduction

Recent interdisciplinary research on hominin activity and habitats during the Plio-Pleistocene is focusing on landscape-scale excavation at Olduvai Gorge, Tanzania (Blumenschine and Masao, 1991; Blumenschine et al., 1997, 1999, 2003). Fieldwork began in 1989, and members of the Olduvai Landscape Paleoanthropology Project (OLAPP) have excavated over 100 trenches throughout a 20-km-wide swath of the paleo-basin since then. The excavations sample a narrow time slice in upper Bed I and lowermost Bed II and contain rich evidence of

the geologic, fossil bone, and stone artifact record in northern Tanzania.

Previous archaeological excavations at Olduvai, which were revolutionary for their time, were mainly limited to large-scale sites from different stratigraphic horizons (Leakey, 1971). These traditional excavations exposed only the densest traces of hominin activity found along the sinuous geologic outcrops within the gorge, and within Bed I and lower Bed II were limited to only one geographic setting, the eastern margin of a small, alkaline lake (Hay, 1976). Thus, the published record of early hominin paleoecology at Olduvai is spatially and geographically biased and places limitations on our ability to reconstruct ancient habitats or the full range of hominin activity within the basin.

The landscape approach was developed by archaeologists, geologists, and paleontologists (e.g., Potts, 1989, 1994; Bown and Beard, 1990; Blumenschine and Masao, 1991; Potts et al.,

* Corresponding author.

E-mail addresses: nsikes@swca.com (N.E. Sikes), gmashley@rci.rutgers.edu (G.M. Ashley).

1999). In Early Stone Age archaeology, this method was preceded by studies of surface scatters and patches in the Turkana Basin (Isaac and Harris, 1980, 1997; Stern, 1993). By detailed characterization of local paleolandscapes with very high time resolution, we can reconstruct the paleoecology and evolution of fossil assemblages. Using this approach, we determine from the geological and pedological record exposed within trenches excavated at Olduvai the spatial, temporal, environmental, and ecological characteristics present in the basin during the late Pliocene and early Pleistocene.

We focus in this paper on the paleoecology of the westernmost extent of the main gorge (Fig. 1). Eleven OLAPP trenches from a 2.5 km² area are the first excavations on the western side of paleo-Lake Olduvai (Blumenschine et al., 2003). The trenches represent a portion of upper Bed I and contain fluvial and lake deposits, volcanic ash, eolian sediment, and paleosols. The data presented here were collected between 1995 and 1999, and do not necessarily reflect observations and interpretations made by OLAPP since that time.

The objectives of the study are to 1) reconstruct the paleoenvironment based on the spatial and temporal distribution of the sedimentary deposits of upper Bed I that overlie Tuff IB (Fig. 2), 2) present stable carbon and/or oxygen isotope values of paleosol carbonate and organic matter from the deposits, and 3) interpret the paleoecology by integrating the two datasets and then placing it into a broader paleoclimatic context. To achieve these objectives, the upper Bed I sediment record is used to reconstruct the spatial distribution of physical features, such as lakes, rivers, and uplands, and to define and trace the finer stratigraphic intervals represented by volcanic tuffs, lake expansion and contraction, river incision, sedimentary deposition, and soil formation. The widely spaced samples of these microstratigraphic units exposed in the trenches also

enable us to examine lateral variation in the local physical or biological features of the paleolandscapes. We use the stable oxygen and carbon isotope values preserved within the carbonate and/or organic components of paleosols (buried soils) to reconstruct local climatic conditions and variation in tropical vegetation communities with different proportions of grasses (C₄) to woody (C₃) vegetation (e.g., Sikes, 1994, 1996; Sikes et al., 1999). This approach recognizes that not even a single paleosol is equivalent to an actual landscape because of the effects of time-averaging (e.g., Potts et al., 1999; Sikes et al., 1999). The study complements previous diachronic isotopic research at Olduvai that included Beds I–IV, among others (Cerling et al., 1977; Cerling and Hay, 1986; also see Cerling, 1992), by providing isotopic data across the upper Bed I landscape. The temporal objective is achieved by combining the detailed mapping and correlation of sedimentary units with the isotopic data from the paleosols to generate a dynamic picture of the Olduvai Basin on a landscape-scale through time. This reconstruction also provides the basis for viewing local paleoenvironmental variation in a global context.

Geologic and geomorphic setting

Olduvai Gorge incises the eastern margin of the Serengeti Plain of northern Tanzania, exposing a 30-km-wide basin of Plio-Pleistocene sediments (Fig. 1). Bed I is at the base of a stratigraphic sequence that comprises a 100-m-thick, two-million-year stack of interbedded tephra and reworked pyroclastic sediments. Late Pleistocene incision by the Olduvai River exposed the deposits, which had accumulated in a shallow sedimentary basin situated on the margin of the East African Rift between Precambrian shield rocks to the west

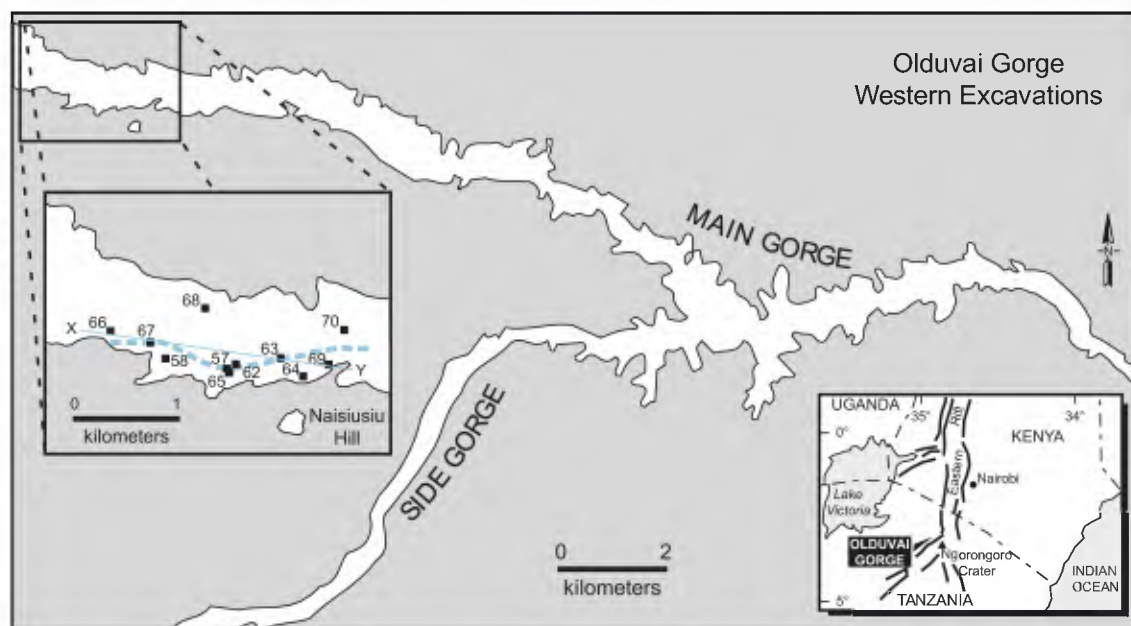


Fig. 1. Olduvai Gorge is located in northern Tanzania (inset map) just west of the Ngorongoro volcanic complex in the East African Rift. The 2.5 km² study area in Bed I is in the westernmost part of the main gorge, and includes 11 step trenches. The trenches are designated by number; the east-west (X–Y) transect is the location for Fig. 6. The dashed line among the trenches represents a channel of a Bed I river flowing from west to east, as interpreted from the sedimentary record.

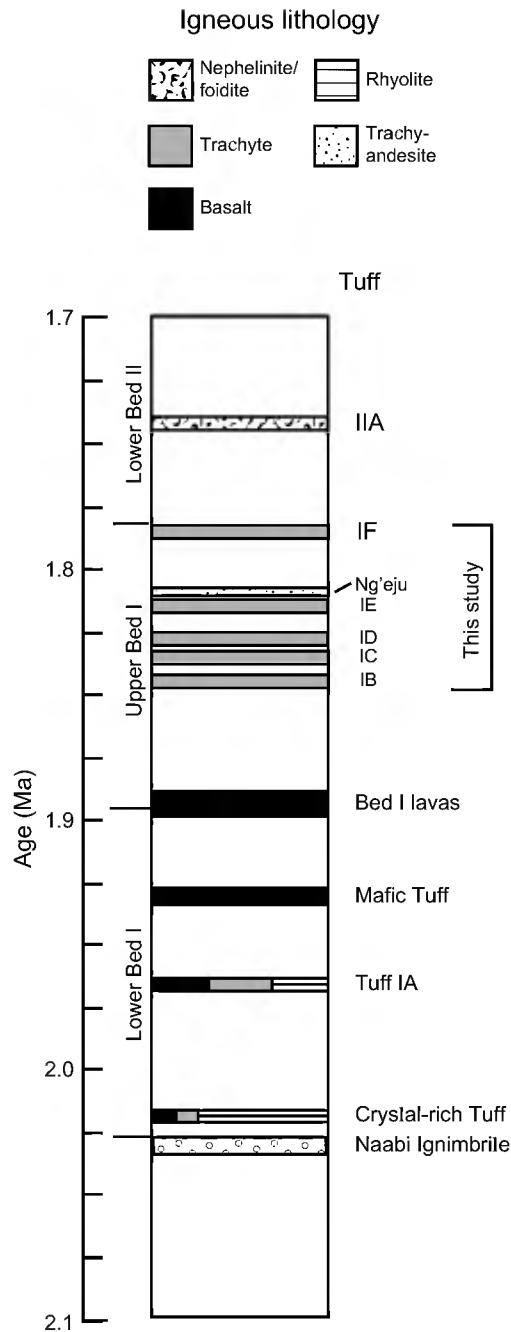


Fig. 2. Tuff stratigraphy, Bed I and Lower Bed II. Geologic section used in this study is indicated. Dates from Hay (1976), Walter et al. (1991), Hay and Kyser (2001), and Blumenschine et al. (2003). Question marks indicate tephra horizons without well-constrained dates. Igneous lithologies based on glass composition from McHenry (2004, 2005).

and a Plio-Pleistocene trachytic volcanic highland to the east (Hay, 1976; Ashley and Hay, 2002). Based on present altitudes and regional geography, the top of the now-extinct volcanoes in the adjacent Ngorongoro complex would have been more than 1,500 m higher than the elevation of the Bed I paleolandscapes, estimated at $\sim 1,500$ m (Fig. 3). During the Plio-Pleistocene, a pyroclastic alluvial fan adjacent to the volcanic highland was created by episodic eruptions that produced

ejecta, which occasionally blanketed the entire basin and formed discrete laterally continuous beds. Many of these tuff beds can be identified by geochemical fingerprints and correlated between isolated outcrops using tephrochronology (McHenry, 2005).

During Bed I times, a small, relatively shallow lake in the center of the Olduvai Basin expanded and contracted, likely responding to both short-term (seasonal) and long-term (Milankovitch-scale) fluctuations in local effective precipitation (Hay, 1976; Ashley and Driese, 2000; Ashley, 2001; Table 1). The time frame of lake fluctuations is based on the lithostratigraphic record that is temporally constrained by $^{40}\text{Ar}/^{39}\text{Ar}$ dating and magnetostratigraphy (Hay and Kyser, 2001; Blumenschine et al., 2003). Surface drainage from the Serengeti Plain, lying immediately to the west, flowed into the basin as shallow rivers (Hay, 1976; Bridge, 2003). The record of this fluvial system outside the basin has been eroded and all that remains are the deposits in the westernmost portion of the main gorge (Fig. 1). The deposits from this western fluvial system are the focus of our paleoenvironmental reconstruction.

The age and duration of upper Bed I above Tuff IB is reasonably well-known (Fig. 2). The interval lies within the type section for C2n, the Olduvai Subchron (a brief paleomagnetic reversal to normal polarity, 1.942 to 1.785 Ma) during the Matuyama Chron (Grommé and Hay, 1971; Tamrat et al., 1995; Lourens et al., 1996; Hay and Kyser, 2001; Blumenschine et al., 2003). Tuff IB has been dated at 1.845 Ma (Blumenschine et al., 2003). Thus, the deposits are no older than ~ 1.845 Ma and no younger than 1.785 Ma, and sample upper Bed I (McHenry, 2005; middle-upper Bed I in Leakey, 1971).

Soil carbonate formation and stable isotope values

Carbonate formation

Pedogenic carbonate (CaCO_3) is typically formed by the downward leaching of dissolved carbonate from the surface and upper soil horizons (“*per descensum* model” of Gondie, 1973), which then precipitates and accumulates in the lower B and upper C soil horizons. The depth of precipitation varies for each soil, and is controlled by soil moisture and texture (Gile et al., 1966; Machette, 1985). Carbonate supersaturation due to soil drying during evapotranspiration is generally considered the primary mechanism for CaCO_3 precipitation (e.g., Jenny, 1980; Cerling, 1984; Quade et al., 1989b), which typically occurs in well-drained soils in the vadose or unsaturated zone above the influence of the groundwater table (Fig. 4A). Where the groundwater table fluctuates on a seasonal basis, pedogenic CaCO_3 may also precipitate in hydromorphic soils at the capillary fringe under the influence of groundwater or in a water saturated state (e.g., Freytag and Plaziat, 1982; Slate et al., 1996). Nonpedogenic, groundwater carbonate forms in the phreatic zone below the top of the groundwater table (Lintkus et al., 2005), or as a capillary rise phenomenon.

Precipitated pedogenic carbonate occurs as discontinuous nodules, calcified root traces (rhizoliths of Klappa, 1980), pendants, laminar coatings, or massive continuous layers that may

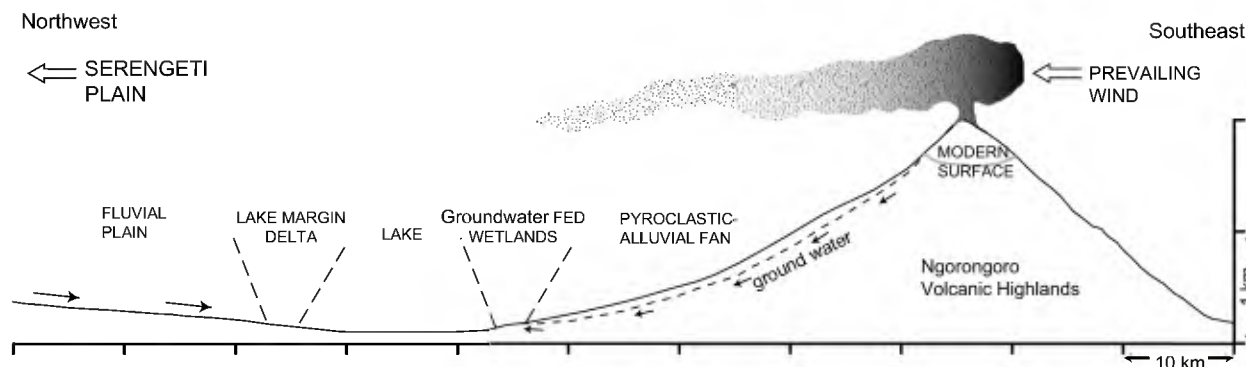


Fig. 3. Reconstruction of a northwest-southeast transect of the Olduvai Basin topography during the Plio-Pleistocene. The Ngorongoro volcanic complex had at least one active volcano that periodically erupted pyroclastic material that was carried westward by the prevailing winds. A lake in the basin center expanded and contracted through time. Rivers drained into the basin from the Serengeti Plain located to the west, and a delta formed at the lake margin. Reconstruction of wetlands in the eastern lake margin is based on evidence uncovered for lowermost Bed II (Ashley and Hay, 2002; Liutkus and Ashley, 2003; Liutkus et al., 2005).

be up to several meters thick (calcrete). Diffuse accumulations of pedogenic carbonate may also be disseminated within the soil profile. The occurrence of soil carbonate is dependent on rainfall patterns, and is typical of areas receiving less than 750–850 mm of annual rainfall, and in soils developed under seasonal wet-dry climates (Birkeland, 1984; Cerling, 1984; Blodgett, 1988; Retallack, 1990; Royer, 1999). Pedogenic calcrete may be common in very arid regions with sparse vegetation cover.

Soil CO₂, the source of carbon in pedogenic carbonate, is comprised of two isotopically distinct sources: 1) biologically-respired CO₂ from plant root respiration and litter decomposition (microbial oxidation) and 2) atmospheric CO₂ (Fig. 4A). The relative contribution of each of these sources to soil CO₂ depends on the production rate of biogenic CO₂,

atmospheric pressure, depth of carbonate precipitation, and soil porosity (Cerling, 1984; Quade et al., 1989b; Cerling and Quade, 1993). Except in sparsely vegetated desert soils, penetration by atmospheric CO₂ is mostly limited to the upper 5–20 cm of the soil column by the high flux of biogenic CO₂ and low diffusivity and porosity. Carbon from detrital, previously formed soil, or parent carbonate (e.g., limestone, marble, calcic rocks) may also be present in a soil; but again, high soil CO₂ respiration rates from the influx of biogenic CO₂ prevent inheritance in discrete, nondisseminated forms of pedogenic CaCO₃, like those analyzed here. The isotopic composition of hydromorphic and groundwater carbonate may be contaminated by non-plant sources of carbon (Quade et al., 1995; Slate et al., 1996; Quade and Roe, 1999), and are not part of this study.

Table 1
Interpreted geological history of western Bed I

Approximate date (Ma) ¹	Interpreted climate ²	Geologic process or event	Lithostratigraphic unit ³	Mean δ ¹⁸ O value ⁴
1.785		top of Olduvai Subchron C2n		
	wet to dry	contraction of lake volcanic eruption	H (tuffaceous claystone) G (Tuff IF)	−4.5‰ (n = 2)
	dry to wet	expansion of lake (minor)	F (tuffaceous claystone)	−4.8‰ (n = 21)
	dry	contraction of lake	E (tuffaceous claystone)	−4.4‰ (n = 10)
	wet to dry	fluvial incision contraction of lake	D (sandstone)	
	wet to dry	volcanic eruption contraction of lake	C (Tuff IC)	
	wet	expansion of lake (major)	B (waxy claystone)	−4.8‰ (n = 7)
1,845	dry	volcanic eruption	A (Tuff IB)	

¹ The stratigraphic interval overlying Tuff IB falls within the type section for the Olduvai Subchron, dated from 1.942 to 1.785 Ma (Grommé and Hay, 1971; Tamrat et al., 1995; Lourens et al., 1996; Blumenschine et al., 2003). Date of ~1.845 for Tuff IB from Blumenschine et al. (2003); identification of Tuff IC and Tuff IF (McHenry, 2004, 2005).

² Relative wetness vs. dryness interpreted from lithologic record.

³ Units are defined in the text, and were assigned a letter from oldest to youngest.

⁴ Derived from paleosol carbonate isotopic data listed in Table 2; descriptive statistics are given in Table 3. Differences in the range of δ¹⁸O values between Units B, E, and F are statistically significant ($P < 0.05$).

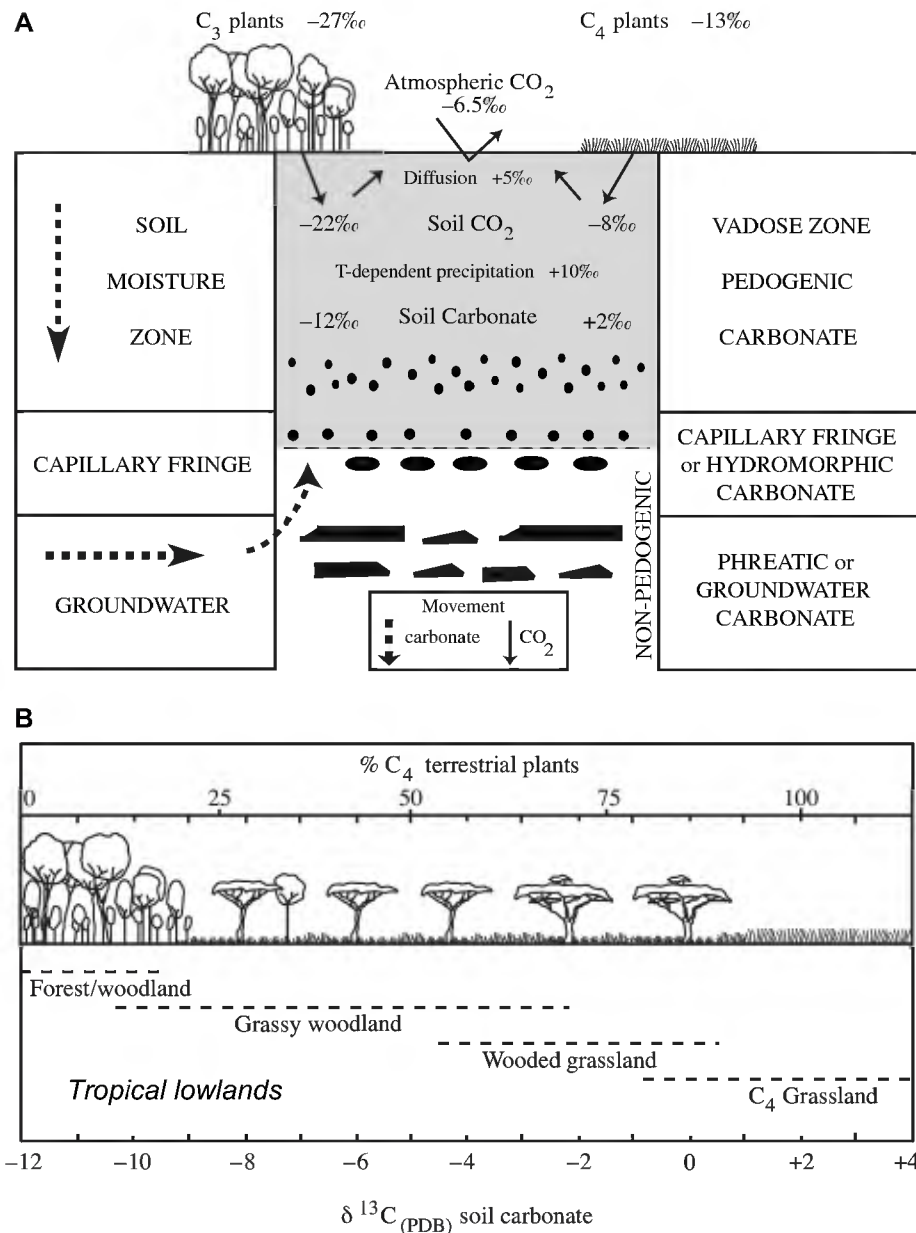


Fig. 4. (A) Pedogenic and nonpedogenic carbonate formation (separated by the horizontal dashed line) relative to movement of aqueous carbonate in soils or groundwater, plus the relationship of pedogenic carbonate formed under or near isotopic equilibrium with plant-derived CO_2 , using $\delta^{13}C$ values for C_3 and C_4 plant means (Deines, 1980), pre-industrial atmospheric CO_2 (Friedli et al., 1986), and resultant precipitated soil carbonate; and (B) modern analog scale used to interpret paleovegetation communities in the tropical lowlands from soil carbonate $\delta^{13}C$ values, showing the approximate equivalent percentage of C_4 plants and the ranges for floral communities after Cerling (1992). Although pedogenic carbonate $\delta^{13}C$ values precipitated beneath 100% C_4 and C_3 biomass reflect variation in equilibrium fractionation factors and range from -12 to -9‰ and $+1$ to $+4\text{‰}$, respectively, the theoretical end-members are set at $+2\text{‰}$ and -12‰ (after Cerling, 1992).

Soil stable isotope values

The stable isotopic composition of pedogenic carbonate is related to the proportion of C_3 and C_4 plant biomass contributing to soil CO_2 (Cerling, 1984; Quade et al., 1989b; Cerling and Quade, 1993). These two groups of plants differentially fractionate against atmospheric $^{13}CO_2$ during photosynthesis, resulting in a bimodal, nonoverlapping distribution of their $\delta^{13}C$ values. Worldwide average $\delta^{13}C$ values for C_3 (-27‰) and C_4 (-13‰) plants are shown on Fig. 4A (Deines, 1980) ($\delta\text{‰} = [R_{\text{sample}}/R_{\text{standard}} - 1] \times 1,000$

where R is the $^{13}C/^{12}C$ or $^{18}O/^{16}O$ ratio, and the standards used here are PDB for carbonate and SMOW for water). C_4 plants follow the Hatch-Slack photosynthetic pathway and include tropical grasses, sedges, and forbs adapted to conditions of water stress, high temperature, and low atmospheric CO_2 concentrations. C_3 plants, which follow the Calvin-Benson pathway, include nearly all trees, shrubs, and forbs, a few sedges, plus grasses adapted to cool growing seasons and shade.

Pedogenic carbonate precipitated in equilibrium with soil CO_2 beneath 100% C_4 vegetation is recorded in $\delta^{13}C$ values

ranging from +1 to +4‰, and from –12 to –9‰ beneath pure C₃ biomass (Cerling, 1984; Cerling et al., 1989; Cerling and Quade, 1993). The spread in pedogenic carbonate $\delta^{13}\text{C}$ values for pure C₃ or C₄ vegetation end-members reflects the variation of the equilibrium fractionation factor with temperature of precipitation in addition to a minimum enrichment of +4.4‰ during upward diffusion of CO₂ from the soil. Fig. 4A illustrates this process using the mean C₃ and C₄ plant $\delta^{13}\text{C}$ values, with isotopic enrichments of +5‰ for diffusion and +10‰ for temperature-dependent equilibration at about 25°C from aqueous soil CO₂ to solid CaCO₃. The resulting pedogenic carbonate values of +2‰ and –12‰ are used as end-members for a modern analog scale showing the approximate equivalent percentage of C₄ plants (Cerling, 1992) (Fig. 4B).

Pedogenic carbonate formed in equilibrium with soil-respired CO₂ is typically enriched in ¹³C by 13.5 to 17‰ over that of the respiring plants, as well as that of decomposing soil organic carbon and related soil organic matter (Cerling, 1984; Cerling et al., 1989; Cerling and Quade, 1993). Pedogenic carbonate and organic matter $\delta^{13}\text{C}$ values have thus been used to 1) determine the proportion of C₄ biomass (0 to 100%) contributing to soil CO₂ and 2) differentiate between standard physiognomic types of tropical plant communities in East Africa (e.g., Cerling, 1992; Kingston et al., 1994; Sikes, 1994, 1995; Sikes et al., 1999). The $\delta^{13}\text{C}$ values of these two soil components increase as tree cover decreases and C₄ biomass increases. This method is demonstrated in Fig. 4B using pedogenic carbonate $\delta^{13}\text{C}$ values.

The standard floral communities illustrated in Fig. 4B are defined by ground and canopy cover (Pratt et al., 1966; Pratt and Gwynne, 1977). Tropical C₄ grasses dominate the continuous herbaceous layer in three structural types of open canopy, vegetational savanna found at low and intermediate altitudes, which also have a clear seasonality of growth related to water stress. These three open-canopy structural types are: 1) grassy woodland (including bushland and shrubland categories) with a canopy cover of >20%, 2) wooded grassland (including bush grassland and shrub grassland categories) with a canopy cover of <20%, and 3) low and intermediate elevation treeless or sparsely treed grassland (including semi-desert dwarf shrub grassland) with a canopy cover of <2%. The discontinuous ground cover in closed canopy forest and near-closed canopy woodland is dominated by C₃ herbs and shrubs. This classification of savanna vegetation has been used to describe and sample modern plants and soils, and is consistent with prior reconstructions of vegetation communities based on buried Holocene age or older pedogenic carbonate or organic $\delta^{13}\text{C}$ values (Ambrose and Sikes, 1991; Cerling et al., 1991; Cerling, 1992; Sikes, 1994, 1995, 1996; Sikes et al., 1997, 1999). A similar classification scheme, also used to interpret paleovegetation from isotopic data (e.g., Wynn, 2000), combines terminology developed by Cole (1963) with annual precipitation and soil drainage and texture to explain the distribution of savanna types (Johnson and Tothill, 1984; Belsky, 1990; Owen-Smith, 1999). In that scheme, with annual rainfall ranging between 400–1,500 mm, savanna woodland (= grassy

woodland) occurs on sandy, well-drained soils, with savanna parkland (= wooded grassland) on less well-drained soils, and savanna grassland (= grassland) on clay-rich, poorly drained soils.

There is a systematic relationship between pedogenic carbonate $\delta^{13}\text{C}$ and $\delta^{18}\text{O}$ values within many areas worldwide (Cerling, 1984; Cerling and Quade, 1993). Pedogenic carbonate $\delta^{18}\text{O}$ values are derived from soil water; soil water is ultimately related to the $\delta^{18}\text{O}$ of meteoric water, which is well-correlated with mean annual air temperature. In general, cooler or moister regions have lower meteoric water and carbonate $\delta^{18}\text{O}$ values than do hot and dry areas. In the tropical lowlands in East Africa today, for example, warm areas with low annual rainfall generally have a greater proportion of C₄ relative to C₃ plant biomass and, thus, higher $\delta^{18}\text{O}$ and $\delta^{13}\text{C}$ values.

By definition, paleosols are buried in their place of formation and, barring other factors, such as inheritance or diagenesis, their $\delta^{13}\text{C}$ and $\delta^{18}\text{O}$ values represent a time-averaged signal of site-specific vegetation and local climatic conditions. These data may be interpreted by comparison with the $\delta^{13}\text{C}$ and/or $\delta^{18}\text{O}$ values of recent soil organic matter and pedogenic CaCO₃ (see Fig. 4B). The C₄ pathway was present in East Africa by at least the middle Miocene (Kingston et al., 1994; Morgan et al., 1994), and there was a global expansion of C₄ biomass between 8–6 Ma (Cerling et al., 1997, 1998). C₃ grass-dominated vegetation belts occur in equatorial Africa today only above 2,700–3,000 m (e.g., Tieszen et al., 1979; Livingstone and Clayton, 1980) and remained above 2200 m during glacial times (e.g., Bonnefille et al., 1990; Taylor, 1992). C₃ photosynthesis may thus be treated as evidence of woody vegetation in interpreting paleosol $\delta^{13}\text{C}$ values at Olduvai and other localities in tropical East Africa at low and intermediate altitudes since C₄ grasses dominate the landscape, with C₃ grasses restricted to cooler, shaded, forest understories or wetlands.

During the past 30 years this method of environmental reconstruction has been applied to early hominin and hominoid localities in East Africa (e.g., Cerling et al., 1977, 1988; Cerling and Hay, 1986; Cerling, 1992; Kingston et al., 1994; Sikes, 1994, 1996, 2000; Sikes et al., 1997, 1999; and summarized in Sikes, 1999), as well as other time periods and areas worldwide (e.g., Quade et al., 1989a, 1995; Smith et al., 1993; Alam et al., 1997). Pedogenic carbonate and organic $\delta^{13}\text{C}$ values represent many generations of plants, averaged over the lifetime of a soil (hundreds or thousands of years). Temporal shifts of C₄ biomass at East African localities have been correlated with change in carbonate $\delta^{18}\text{O}$ values (e.g., Cerling, 1992; Cerling and Hay, 1986; Cerling et al., 1988; Sikes et al., 1997).

Materials and methods

Field sampling

The isochronostratigraphic deposit Tuff IB was traced throughout the 2.5 km² study area (Fig. 1). Eleven step trenches were placed with Tuff IB at the base and extending

upward to at least a thin pumice lapilli layer that was visible in most exposures. The lapilli-rich unit was interpreted to be an isochronostratigraphic deposit that correlated geochemically to Tuff IF (Blumenschine et al., 2003; McHenry, 2005) thus putting an age limit to the “time-slice” under study.

The trenches are 1–2 m wide and expose a vertical stratigraphy up to 6 m in height. The lithology was logged (bedding, sedimentary structures, pedogenic features, color). Representative sediment samples and pedogenic carbonate were collected in conjunction with stone artifacts and fossil bones. We report here only the lithologic and stable isotope results, including isotopic data on local modern soils. An example of a detailed log of one of the trenches (Trench 62) with stratigraphy and sample locations is depicted in Fig. 5.

Geological fieldwork attests to the absence of a local carbonate reservoir; hence, inheritance of inorganic $\delta^{13}\text{C}$ values from detrital or parent material is not an issue for interpretation of the Bed I paleosol carbonate isotopic data. Calcareous rocks, which can be potential contributors of carbonate, are not known in the source area (Hay, 1976). Nor has natrocarbonate ash been recorded at Olduvai prior to deposition of the Masek Beds ~ 0.6 Ma (Hay, 1976) despite the occurrence of this carbon-rich ash only ~ 45 km to the southwest at Laetoli within deposits dated at ~ 3.6 to 2.4 Ma (Hay, 1987). In addition, only discrete forms of pedogenic CaCO_3 (nodules, rhizoliths, and calcrete) were included in the paleosol study. Inheritance of detrital, previously formed soil, or parent carbonate within such forms has been shown to be minimal where plant respiration rates in the soil system are high (Cerling, 1984; Hay, 1989; Quade et al., 1989b; Cerling and Quade, 1993). The size of the nodules and rhizoliths ranges from 0.5–3 cm in diameter. A thin calcrete, traced within Trenches 57 and 62 and a nearby geologic profile, has a maximum thickness of 10 cm.

Stable isotope and petrographic analyses

Three components from the Bed I paleosols and local modern soils were analyzed: pedogenic carbonate, organic matter occluded within the paleosol and soil carbonates, and disseminated organic matter from one modern soil (Table 2). Standard petrographic analysis was performed on select paleo- CaCO_3 samples ($n = 10$) prior to geochemical preparation. As expected for pedogenic carbonate precipitated in the vadose zone (e.g., Cerling, 1984; Quade et al., 1995), micritic calcite was dominant in the thin sections. All carbonate was cleaned and oven dried at 70°C before drilling or grinding. After drying overnight at 90°C , 9 to 19 mg of CaCO_3 powder was reacted with 100% H_3PO_4 in vacuo at 50°C for 15 hours. CaCO_3 was not roasted since there is no significant difference in $\delta^{13}\text{C}$ and $\delta^{18}\text{O}$ values between roasted vs. unroasted pedogenic carbonate reacted with acid prepared without CrO_3 (Marion et al., 1991; Sikes et al., 1999; N.E. Sikes, unpublished data). Modern rootlets were hand-picked from the bulk soil prior to gentle grinding and sieving ($<355 \mu\text{m}$), followed by reaction with 1 M HCl to remove any carbonate. After reaction ceased, the material was rinsed with distilled water

and lyophilized, before combustion at 900°C with Cu granules, CuO wire, and Ag foil. The evolved CO_2 gas from the carbonate reactions and organic combustion was purified and measured before collection; carbon and oxygen isotopic ratios were then measured on a Finnigan Delta-E mass spectrometer.

For analysis of occluded organic matter, first the carbonate matrix was removed by reacting 3 to 3.5 g of ground powder in 10% HCl for 24 hours. After reaction ceased, all carbonate-free material was rinsed with distilled water, followed by lyophilization. Isotopic ratios for the dry, treated material were obtained from an automated system, with a Carlo Erba 2500 elemental analyzer in direct connection to a Finnigan MAT 252.

All isotope values are reported in the usual delta (δ) notation as parts per mil (‰) relative to the Pee Dee belemnite (PDB) standard. Analytical precision is better than $\pm 0.2\text{‰}$.

Statistical analysis

The paleosol carbonate $\delta^{13}\text{C}$ and $\delta^{18}\text{O}$ values were each grouped by stratigraphic unit ($n = 4$) and depositional environment (facies; $n = 4$), then further grouped by facies within Units E ($n = 3$), F ($n = 3$), and H ($n = 2$). Groups with a sample size of two or less were excluded from the statistical tests. The significance of any temporal or spatial variation in the inter unit, inter facies, or intra unit groups was compared using the one-way analysis of variance (ANOVA) and the nonparametric Kruskal-Wallis test. If there were any significant differences at the $P < 0.05$ level, standard t-tests and the Tukey HSD (honestly significant difference) test were used to compare means among the grouped data.

Stratigraphy and sedimentology

Description of sediments

Eight distinctive lithostratigraphic units can be traced throughout the study area: Unit A (Tuff IB), Unit B (green waxy claystone), Unit C (gray silty tuff), Unit D (medium-coarse sandstone), Units E and F (tuffaceous claystones with a wide range of physical characteristics), Unit G (pumice lapilli layer), and Unit H (tuffaceous claystone) (Fig. 6). The oldest unit (Tuff IB) is a pyroclastic deposit. It is a thin (20–30 cm), highly weathered trachyte, and occurs in all trenches. The green waxy claystone (20–120 cm) pinches out to the west (it is not present at Trench 66); the gray silty tuff (75 cm) pinches out to the east (it is not present at Trenches 63, 64, 69, and 70), although this tuff was later found to be an equivalent of Tuff IC (McHenry, 2004, 2005). A medium-coarse quartzofeldspathic sandstone overlies these two units at Trench 58. At other places the sandstone directly overlies the gray silty tuff (Trench 66), the green waxy claystone (Trench 63), or Tuff IB (Trenches 57 and 65), or does not occur at all in the section (Trenches 62 and 69). A thick sequence of tuffaceous claystones, which are sandy or silty near the base, overlies the sandstone. Sand is restricted to the base of the tuffaceous claystones and is present at only a few trenches

	STRATIGRAPHY	LITHOLOGIC DESCRIPTIONS	LITHOLOGY SAMPLES	ISOTOPE SAMPLES	UNITS
6.0	TUFFACEOUS CLAYSTONE	2.5Y 3/2 insect traces	GA-15-96	NS-224	H
	TUFF IF	pumice lapilli layer	GA-T-8-96		G
5.0	BROWN WAXY CLAYSTONE	2.5Y 4/3 olive-brown widely dispersed nodular concretions black (Mn?) aureoles	GA-16-96	NS-225	F
	CALCRETE		GA-17-96	NS-226	
	BROWN WAXY CLAYSTONE	10YR 3/1 Mn stain prismatic soil structure	GA-18-96		
4.0	BROWN WAXY CLAYSTONE	2.5Y 4/4 olive brown massive, insect traces lined with blue/gray/black, random calcareous concretions (1 cm)	GA-19-96	NS-239 NS-229	E
3.0	BROWN SILTY WAXY CLAYSTONE	2.5Y 5/3 lt olive-brown silty, highly calcareous, insect traces and roots? partially lined with calcite	GA-20-96		
	VERY FINE SAND	sand includes pumice	GA-21-96		
2.0	BROWN SILTY WAXY CLAYSTONE	2.5Y 6/3 lt yellow-brown tubules (root?) and cracks partially filled with calcite		NS-230	C
1.0	GRAY SILTY TUFF	5Y 6/2 lt olive-gray stratified, very well sorted silty ash with calcareous nodules (0.5 cm)	GA-25-96		
	TUFF IC		GA-26-96		
	GREEN WAXY CLAYSTONE	2.5Y 4/2 dark gray brown no insect traces black nodules (0.5 cm)	GA-27-96	NS-233	B
0.0	TUFF IB	weathered tuff	GA-T-19-96 GA-T-20-96		A

Fig. 5. Lithologic description of Trench 62, a six-meter-long step trench excavated above Tuff IB that exposed a sequence of units that could be correlated to other trenches. Location of samples collected for lithologic and stable isotope analyses are indicated. The geographic location is shown on Fig. 1. Lithologic descriptions include Munsell soil color description codes.

(57, 58, 65). The silt content everywhere decreases upward through the 6 m section. The tuffaceous claystones have pumice and lapilli and are comprised of discrete beds 10–120-cm-thick (Fig. 5). The Unit G pumice lapilli layer that was later correlated with Tuff IF (McHenry, 2004, 2005), occurs between 5–6 m above Tuff IB in most trenches.

All sedimentary units have weakly developed paleosols, which ranged in thickness from 0.6 to 1.2 m. Abundant physical evidence of pedogenesis includes prismatic and blocky peds, microcracks, and root and/or insect traces lined with calcite, as well as micritic pedogenic carbonate. In addition, calcareous nodules and rhizoliths, manganese nodules and staining, and a calcrete indicate soil formation in the basin on riverine floodplains, interfluvies, and the former lake bottom after recession or desiccation of the lake waters. The paleosols are immature with no visible horizonation, which suggests a recurring influx of

sediment into the basin resulted in relatively little time for mature soil development. Although the weakly developed paleosols have little to no evidence of horizonation, the abundant insect and root traces indicate they were not sparsely vegetated desert soils at the time of soil formation. Pedogenic carbonates were collected at depths ranging from 0.2–2.6 m below the top of Units B, C, E, F, and H (Table 2), illustrated on Fig. 6 with the isotope sample numbers from Trench 62. The depth of the groundwater table at the time of soil formation is estimated to be 2 m or more based on modern analogs in East Africa (G.M. Ashley, unpublished data).

Interpretation of the geological history

The geological history is interpreted from physical characteristics of the stratigraphic units and the spatial (lateral and

Table 2
Stable isotopic composition of soil carbonate and organic matter from western upper Bed I paleosols and modern soils

Trench or locality ¹	Sample no. ²	Soil carbonate		Form ³	Depth (m) ⁴	Soil organic matter		Unit ⁶	Depositional environment ⁷	Plant community ⁸
		$\delta^{13}\text{C}$	$\delta^{18}\text{O}$			$\delta^{13}\text{C}$	SOM Δ^5			
<i>Upper Bed I paleosols</i>										
62	NS-224-96	-4.4	-4.4	N	0.25	-22.3	17.9	H	floodplain	GW/WG
62	NS-225-96	-4.2	-4.7	N	0.30			F	floodplain	GW/WG
62	NS-226-96	-4.6	-4.3	C	0.80			F	floodplain	GW
62	NS-239-96	-4.3	-4.9	N	1.45			F	floodplain	GW/WG
62	NS-229-96	-4.3	-4.8	N	2.10	-19.5	15.3	F	floodplain	GW ⁸
62	NS-230-96	-4.3	-4.5	N	1.30			E	floodplain	GW/WG
62	NS-233-96	-5.2	-4.3	N	0.30			B	lacustrine	GW
63	NS-243-96	-4.4	-4.3	N	0.65			F	floodplain	GW/WG
63	NS-245-96	-3.3	-3.8	N	0.25	-19.9	16.5	E	floodplain	GW ⁸
63	NS-246-96	-5.7	-4.6	N	0.60			E	floodplain	GW
63	NS-247-96	-4.8	-4.3	N	0.85	-18.6	13.8	E	floodplain	GW
63	NS-248-96	-4.8	-4.6	N	0.20	-19.1	14.4	B	lacustrine	GW
64	NS-267-96	-5.8	-4.6	N	0.25			F	lake margin	GW
64	NS-269-96	-6.4	-4.7	N	1.20			F	lake margin	GW
64	NS-265-96	-5.2	-4.5	N	1.50			F	lake margin	GW
64	NS-266-96	-5.7	-4.8	R	1.85			F	lake margin	GW
64	NS-270-96	-5.4	-4.3	N	0.25			E	lake margin	GW
64	NS-271-96	-5.8	-4.8	N	1.20			E	lake margin	GW
64	NS-272-96	-5.6	-5.2	N	0.30			B	lacustrine	GW
Geo-57a	NS-283-96	-4.2	-4.4	N	0.45			F	floodplain	GW/WG
57	GA-104-96	-4.8	-5.0	C	1.00			F	floodplain	GW
Geo-1B-96	NS-259a-96	-4.6	-4.6	C	0.80			F	floodplain	GW
57	NS-286-96 (avg)	-6.6	-4.7	N	2.60			F	floodplain	GW
Geo-1A-96	NS-254-96	-5.0	-4.8	N	0.20			B	lacustrine	GW
67	NS-294-96	-4.7	-4.2	N	0.40			F	floodplain	GW
67	NS-295-96	-4.3	-5.1	N	1.20			F	floodplain	GW/WG
67	NS-296-96	-4.3	-3.9	N	0.25			E	floodplain	GW/WG
67	NS-297-96 (avg)	-5.6	-4.3	N	0.85			E	floodplain	GW
67	NS-299-96 (avg)	-4.2	-5.0	N	0.20			B	lacustrine	GW/WG
67	NS-300-96	-4.7	-4.6	N	0.25			B	lacustrine	GW
66	NS-301-96	-4.0	-4.7	N	0.35			H	interfluvial	GW/WG
66	NS-302-96	-4.9	-4.3	R	0.25			F	interfluvial	GW
66	NS-303-96	-4.2	-5.5	N	1.35			F	interfluvial	GW/WG
66	NS-304-96	-4.6	-4.4	N	0.40			E	interfluvial	GW
66	NS-305-96	-4.9	-5.1	N	0.50			E	interfluvial	GW
68	NS-306-96	-5.7	-4.9	N	0.45			F	interfluvial	GW
68	NS-307-96	-4.0	-5.6	N	0.75			F	interfluvial	GW/WG
68	NS-308-96	-4.7	-5.0	N	0.95			F	interfluvial	GW
68	NS-309-96	-5.1	-5.3	N	1.50			F	interfluvial	GW
68	NS-311-96	-4.4	-5.5	N	0.20			B	lacustrine	GW/WG
<i>Modern Soils</i>										
Olduvai (Naisiusiu Hill)	NS-313-96	0.6	-1.1	C	S	-14.4	15.1			Modern G
Olduvai (THC)	NS-363-97 (avg)	-0.8	0.8	C	S					Modern G
Lake Masek	SG-3-94	1.5	0.8	C	S					Modern G
Olduvai (Kelogi)	SG-10-94	2.0	1.0	C	S	-15.6	17.6			Modern G
Olduvai	Cerling, 1984: Table 1	0.5	0.3	C						Modern G
Olduvai	Cerling and Hay, 1986: Table 1	0.6	0.2	C						Modern G
Lake Kwennia (Kenya)	NS-O-287-98	-1.6	0.4	D	0.35	-16.0	14.4			Modern WG

¹ Upper Bed I paleosols were analyzed from Trenches 57, 62, 63, 64, 66, 67, and 68, plus three geologic (Geo) sections near Trench 57; samples are listed from the top to the bottom within each trench. Modern soil carbonates reported here (n = 5) include three areas at Olduvai: Naisiusiu Hill to the west (Fig. 1), THC to the east near the Third Fault, and Kelogi at the south end of the Side Gorge (see Hay, 1976); and Lake Kwennia, Olorgesailie Basin, Kenya. Also listed are published values for recent Olduvai calcretes (n = 2), which are included in the Fig. 10 dataset.

² Collected by Sikes (N.S.) or Ashley (G.A.); modern Serengeti (SG) collected by Sikes. For three samples, the isotopic data have been averaged from duplicate runs (avg).

³ Three forms of Bed I paleosol carbonate were analyzed: calcretes (C; n = 3), nodules (N; n = 35), and rootcasts (R; n = 2). Modern carbonates include calcretes from the Olduvai area (n = 6) and disseminated carbonate from Lake Kwennia (n = 1).

⁴ Depth of paleosol carbonate measured from top of Unit B, E, F, or H. Depth of modern Lake Kwennia carbonate measured from soil surface. Modern calcretes were collected from the surface (S).

⁵ $\text{SOM}\Delta = \delta^{13}\text{C}(\text{soil carbonate}) - \delta^{13}\text{C}(\text{soil organic matter})$. Measured occluded organic matter on all paleosol (n = 5) and one modern sample (Naisiusiu Hill); disseminated organic matter on two modern samples (Kelogi and Lake Kwennia).

⁶ Refers to lithostratigraphic units (B, E, F, and H) defined in the text.

⁷ Depositional environment (facies) based on geological characteristics, as defined in the text.

⁸ Grassy woodland (GW); grassy woodland/wooded grassland (GW/WG); C₄ grassland (G); wooded grassland (WG). Compare Bed I paleosol carbonate $\delta^{13}\text{C}$ values to Figs. 4B, 8, 9. For interpretation of NS-229-96 and NS-245-96, soil organic carbon analog scale published by Sikes (1994; Fig. 1) was used, as explained in the text.

vertical) distribution of the deposits (Table 1; Fig. 6). Tuff IB (Unit A) was ejected from one of the volcanic centers (perhaps Olmoti) in the Ngorongoro Volcanic Complex (Hay, 1976). The tuff can be traced throughout the basin and thus appears to have blanketed the landscape, falling into the lake and onto the exposed land surface surrounding the lake. Later lake expansion deposited green waxy claystone (Unit B) over the tuff, but did not reach westernmost Trench 66 (Figs. 1, 6). The lake then began to recede, followed by soil formation prior to an explosive volcanic eruption that spread a fine-grained (silty) gray tuff across the landscape. The tuff is geochemically correlated with Tuff IC on the eastern side of the paleolake (Blumenschine et al., 2003; McHenry, 2005).

As the lake continued to recede, a river system developed and incised locally into the soft underlying substrate, completely removing Tuff IC at Trenches 67 and 63 and cutting down to Tuff IB at Trenches 57 and 65 (Figs. 1, 6). The river was approximately 50 m wide—active channel, 100 m wide (dry period floodplain), and 200 m wide (wet period floodplain)—(Fig. 7). The medium-coarse quartzofeldspathic sandstone (Unit D) was deposited in the active channel, silty tuffaceous claystone (Unit E) on the interfluvies, and brown waxy claystone (Unit F) on the floodplain. Interpretation of the area covered by flooding (floodplain) during dry periods is based on the sediment record (brown waxy claystone). The area ascribed to the wet period floodplain (Fig. 7) is conjectural, but is based on observations of modern surface conditions in the Olduvai drainage when large areas of low

topography were under water from El Niño-related monsoon rains (1997/1998).

With time, the river stopped flowing and both the interfluvial areas and the river valley were gradually covered with tuffaceous claystone (Units E, F, and H). Based on the presence of friable lapilli, some of the tuffaceous material appears to have come directly from erupting volcanoes. Most of the tuffaceous claystone, however, is likely to have been reworked from the pyroclastic fan and lake-margin flats and transported westward by the prevailing trade winds to the fluvial plain (Hover and Ashley, 2003; Fig. 3). Soils then developed on these tuffaceous claystones at a number of localities. The development of soils strongly suggests that the tuffaceous claystones in Units E, F, and H accumulated over a relatively long period of time (a few to tens of thousands of years; Ashley and Driese, 2000).

Results of isotope analyses

Paleosol carbonate nodules ($n = 35$), rhizoliths ($n = 2$), and calcrete ($n = 3$) were analyzed from seven (57, 62, 63, 64, 66, 67, and 68) of the 11 trenches excavated into upper Bed I, and from three geologic sections near Trench 57 (Table 2). Coexisting organic carbon ($n = 5$) was analyzed from Trenches 62 and 63. The isotopic data are best examined temporally by stratigraphic unit and spatially by depositional environment (Table 3; Figs. 8, 9). Paleosol CaCO_3 is grouped by four of the stratigraphic units: B, E, F, and H. Four main facies—interfluvial,

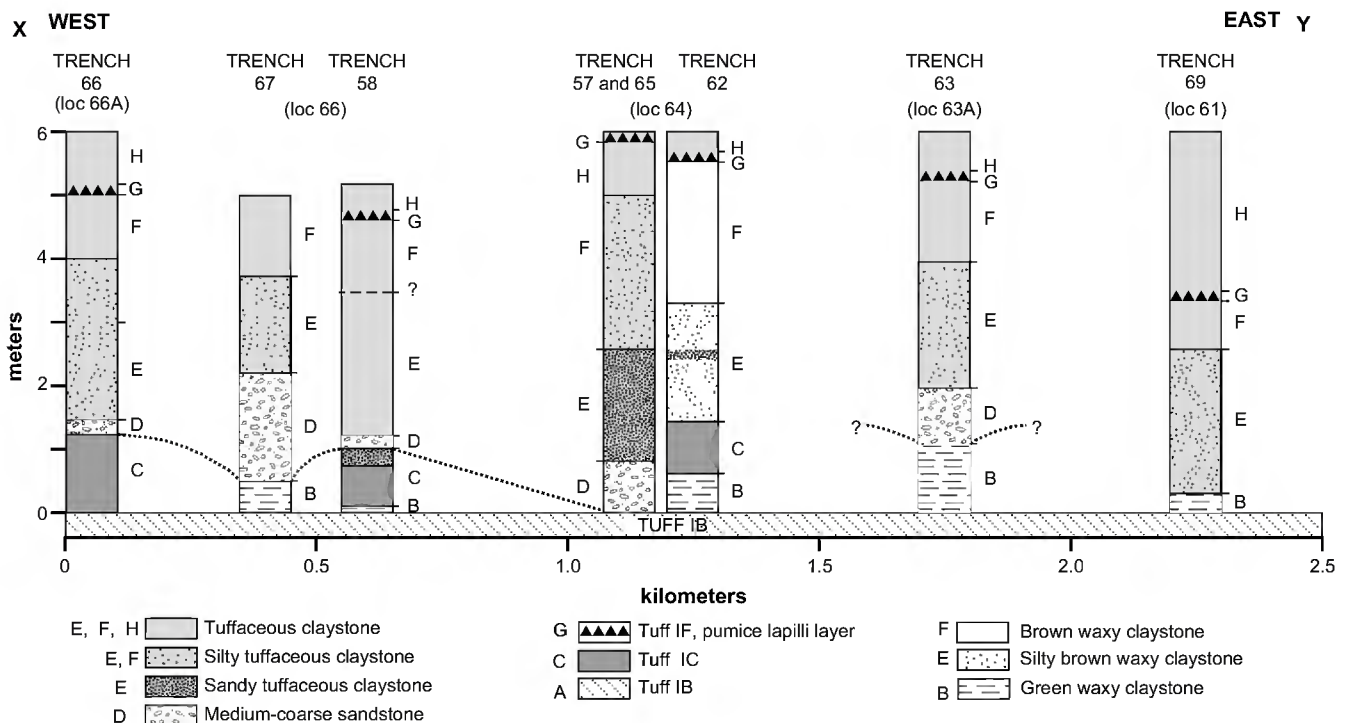


Fig. 6. Fence diagram showing the stratigraphy of upper Bed I as determined by physically tracing the major lithologic units (A through H) between trenches. The fence diagram was drawn assuming Tuff IB was a horizontal surface whereas it probably sloped gently east toward the center of the Olduvai Basin. Green waxy claystone thickens to the east, and the gray silty tuff (Tuff IC) blanketed the westernmost land surface, but either pinches out, was eroded, or was substantially altered to the east (McHenry, 2005). The river incised locally through Tuff IC and at some localities (Trench 57) cut completely down to Tuff IB. The overlying tuffaceous claystone becomes less silty up-section. Fig. 1 gives the location of this east-west transect (X-Y). Geologic localities (loc) after Hay (1976).

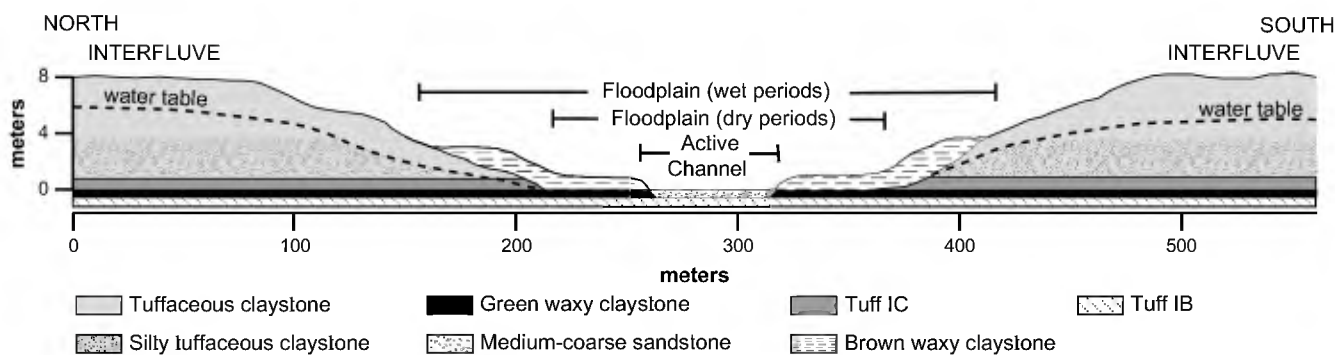


Fig. 7. Diagram depicting the paleotopography of the western Bed I river valley as interpreted from field relationships. The position of the active channel is shown on Fig. 1. It was probably not more than 50 meters wide, whereas the intermittently flooded areas might have been 100 to 200 meters wide.

lacustrine, lake margin, and valley floodplain—are present in the western Bed I excavations. The floodplain and interfluvial facies are represented in Units E, F, and H. The lake-margin facies is present only in Trench 64 and is represented in Units E and F. The lacustrine facies (green waxy claystone) is equal to Unit B. Seven datapoints from the Unit B facies present within six trenches were included in a recent publication on the OH (Olduvai Hominin) 65 *Homo habilis* maxilla recovered from Trench 57 in 1995, providing a general environmental background to the discovery (Blumenschine et al., 2003).

Formation and diagenesis

Two lines of evidence indicate the Bed I pedogenic carbonates precipitated within the vadose zone. None of the paleosols show evidence for greyed coloration or mottling typical of saturation or prolonged seasonal fluctuations of the water table even though the Bed I sediments are relatively fine grained and hence suitable for facilitating capillary rise. Second, the low-lying lake-margin and valley floodplain carbonates in Units E and F are not lower in $\delta^{18}\text{O}$ than their interfluvial counterparts, a result which would be expected if groundwater level had been relatively high and the carbonates formed under less-evaporative hydromorphic conditions (see e.g., Slate et al., 1996). Although the original soil surfaces are not clearly visible in the field, the depth of paleosol carbonate collection below the tops of Units B, E, F, and H (0.2–2.6 m), indicates precipitation likely occurred below soil depths in which soil-respired CO_2 dominates (>20 cm). If atmospheric CO_2 had contributed to any of the paleosol isotopic values reported here, then we would expect at least a portion of the $\delta^{13}\text{C}$ and $\delta^{18}\text{O}$ values to be much more positive, as demonstrated for recent Great Basin soil CaCO_3 (Quade et al., 1989b).

Agreement with a 13.5 to 17‰ range of difference between pedogenic carbonate and organic $\delta^{13}\text{C}$ values found in modern soils (e.g., Cerling et al., 1989; see also Table 2) indicates that the material analyzed from Bed I has not undergone diagenesis. The difference between $\delta^{13}\text{C}$ values for paired carbonate and occluded organic carbon preserved within the CaCO_3 nodules, ranges between 13.8 and 16.5‰, averaging $15.0 \pm 1.2\%$ for four paleosols (Table 2). At 17.9‰, the range of difference for a fifth sample (NS-224-96) is slightly greater than

theoretically expected. Recent research suggests paired $\delta^{13}\text{C}$ values that fall outside the 13.5 to 17‰ theoretical envelope may be related to a seasonal difference in contribution by C_3 or C_4 plants (Wang and Follmer, 1998).

The independent formation and unaltered condition of the paleosol carbonate isotope values from Bed I are further supported by the data shown in Fig. 10. $\delta^{13}\text{C}$ and $\delta^{18}\text{O}$ values from the Bed I carbonates are significantly distinct ($P < 0.0001$) from 1) euhedral calcite crystals precipitated in the center of the paleolake during Beds I and II (Hay, 1976; Cerling and Hay, 1986) and 2) modern soil CaCO_3 in the Olduvai region (Table 2). The higher carbon and oxygen isotope values for the paleolake carbonates are indicative of evaporative conditions in alkaline waters. Indeed, the paleolake $\delta^{13}\text{C}$ values are higher than the theoretical range for pedogenic carbonates formed under a pure C_4 biomass (+1 to +4‰). $\delta^{13}\text{C}$ and $\delta^{18}\text{O}$ values from the modern soil carbonates reflect the dominance of C_4 grasses in the area today and the highly evaporated waters of East Africa, respectively (see e.g., Cerling, 1984; Cerling et al., 1988; Cerling and Quade, 1993). Fossil pedogenic CaCO_3 would approach these higher modern soil carbonate $\delta^{13}\text{C}$ and $\delta^{18}\text{O}$ values if affected by recent diagenetic processes, a factor which is unlikely in today's semi-arid climate.

Carbon isotopes

$\delta^{13}\text{C}$ values for the paleosol CaCO_3 have a fairly narrow range of variation, from -6.6 to -3.3% , with a mean of -4.8% ($n = 40$; Tables 2, 3; Figs. 8, 9), for the entire Bed I interval. Lateral variation in $\delta^{13}\text{C}$ values is typical of soils at comparable altitudes in East Africa and reflects the distribution of C_3 and C_4 plants along a landscape. About 50% C_4 plants are represented by the mean of the dataset; this percentage increases with increase in $\delta^{13}\text{C}$ values. The data indicate that a local biomass of about 40–60% C_4 plants was present at Olduvai during the periods of pedogenic carbonate formation analyzed here. Comparison of the $\delta^{13}\text{C}$ values (grouped by the main depositional environments) indicates the spatial data are significant. Analysis of the carbon data grouped by stratigraphic unit indicates there was little change in the proportion of C_4 biomass through time.

Table 3
Descriptive statistics for western upper Bed I paleosol carbonates grouped by temporal unit, depositional facies, and facies within Units E and F

Group	n	$\delta^{13}\text{C}$ min	$\delta^{13}\text{C}$ max	$\delta^{13}\text{C}$ mean	$\delta^{13}\text{C}$ s.d.	$\delta^{18}\text{O}$ min	$\delta^{18}\text{O}$ max	$\delta^{18}\text{O}$ mean	$\delta^{18}\text{O}$ s.d.
All	40	-6.6	-3.3	-4.8	0.7	-5.6	-3.8	-4.7	0.4
<i>Units</i>									
H	2	-4.4	-4.0	-4.2	0.3	-4.7	-4.4	-4.5	0.2
F	21	-6.6	-4.0	-4.9	0.8	-5.6	-4.2	-4.8	0.4
E	10	-5.8	-3.3	-4.9	0.8	-5.1	-3.8	-4.4	0.4
B	7	-5.6	-4.2	-4.8	0.5	-5.5	-4.3	-4.8	0.4
<i>Facies</i>									
Interfluvial	9	-5.7	-4.0	-4.7	0.6	-5.6	-4.3	-5.0	0.5
Floodplain	18	-6.6	-3.3	-4.6	0.7	-5.1	-3.8	-4.5	0.3
Lake margin	6	-6.4	-5.2	-5.7	0.4	-4.8	-4.3	-4.6	0.2
Lacustrine (Unit B)	7	-5.6	-4.2	-4.8	0.5	-5.5	-4.3	-4.8	0.4
<i>Unit F facies</i>									
Interfluvial	6	-5.7	-4.0	-4.8	0.6	-5.6	-4.3	-5.1	0.5
Floodplain	11	-6.6	-4.2	-4.6	0.7	-5.1	-4.2	-4.6	0.3
Lake margin	4	-6.4	-5.2	-5.8	0.5	-4.8	-4.5	-4.7	0.1
<i>Unit E facies</i>									
Interfluvial	2	-4.9	-4.6	-4.7	0.2	-5.1	-4.4	-4.8	0.5
Floodplain	6	-5.7	-3.3	-4.7	0.9	-4.6	-3.8	-4.2	0.3
Lake margin	2	-5.8	-5.4	-5.6	0.3	-4.8	-4.3	-4.6	0.4

The differences between $\delta^{13}\text{C}$ values for the four facies (Fig. 8) within the Bed I deposits are statistically significant ($P < 0.01$). Valley floodplain carbonates have the widest range in $\delta^{13}\text{C}$ values (-6.6 to -3.3‰, averaging -4.6‰, $n = 18$). $\delta^{13}\text{C}$ values vary the least for Trench 64 lake-margin paleosols (-6.4 to -5.2‰, mean of -5.7‰, $n = 6$), with an intermediate range for Unit B lacustrine

(-5.6 to -4.2‰, mean of -4.8‰, $n = 7$) and interfluvial facies (-5.7 to -4.0‰, averaging -4.7‰, $n = 9$). Three endpoints (-6.6‰, -6.4‰, and -3.3‰) represent vegetation variability on the floodplain and lake-margin soils in three different trenches.

The statistical data are significant for the facies $\delta^{13}\text{C}$ values, but the estimated percentages of C_4 biomass among the facies have only a narrow range of variation (compare Figs. 4B, 8). The floodplain facies supported the greatest range in C_4 biomass, approximating 40–60%, while the $\delta^{13}\text{C}$ values

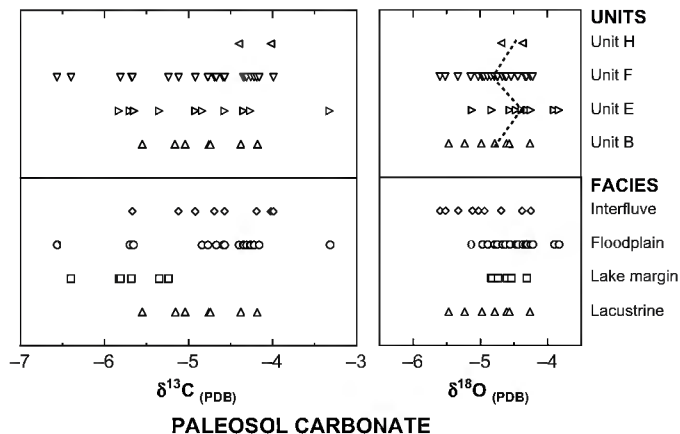


Fig. 8. Stable carbon and oxygen isotopic composition of upper Bed I carbonates precipitated during soil formation, plotted across the landscape by facies (interfluvial, lake-margin, lacustrine, and valley floodplain), and temporally by lithologic units (B, E, F, H). Unit B is equal to the lacustrine facies. $\delta^{13}\text{C}$ values correspond to variation in the proportion of C_4 grasses (~40–60%) and grassy woodland to wooded grassland (see Fig. 4B). All lake-margin paleosols, interpreted as grassy woodland with about 50–60% C_3 plants, are from Trench 64. Significant variation in $\delta^{18}\text{O}$ values indicates precipitation decreased from Unit B to Unit E, with a return to a wetter climate in Unit F; the dotted line connects the mean values tracking lake expansion and contraction, also interpreted from the geologic history summarized in Table 1. Variation in $\delta^{18}\text{O}$ values is also significant between facies, suggesting either evaporation was greater on the floodplains or soil water residence time less on the interfluvies. Limited Unit H data suggest a change in climate and % C_4 ground cover. Data from Table 2.

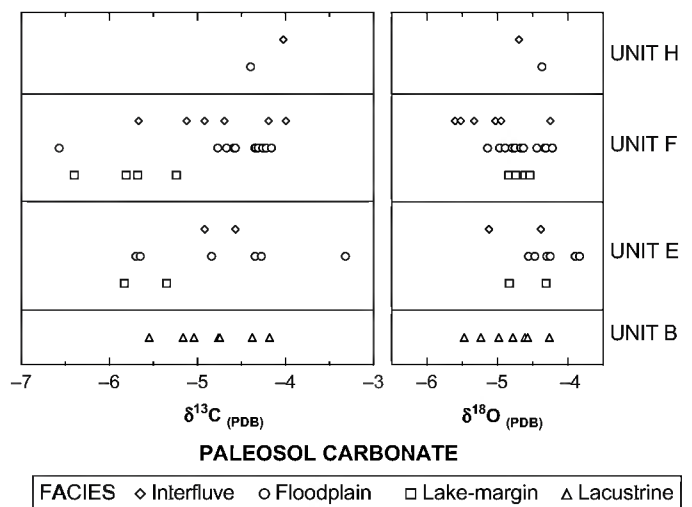


Fig. 9. Stable carbon and oxygen isotopic composition of upper Bed I paleosol carbonates plotted by facies within each stratigraphic unit. Across the time-averaged paleolandscapes within Units E and F, C_4 vegetation is less abundant on the lake-margin soils (~40–50%) compared to other facies; the majority of floodplain carbonate $\delta^{13}\text{C}$ values in Unit F represent >50% C_4 plants (compare with Fig. 4B). Unit F interfluvial $\delta^{18}\text{O}$ values are significantly lower than floodplain and lake-margin facies; the Unit E pattern is similar. This within-facies pattern is analogous to the significant differences in $\delta^{18}\text{O}$ values between the summary facies shown in Fig. 8. Data from Table 2.

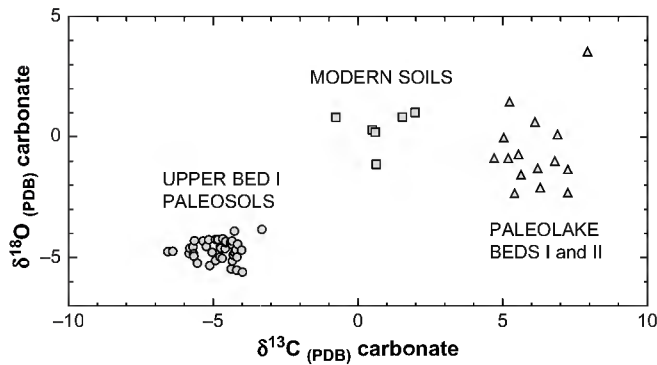


Fig. 10. Stable carbon and oxygen isotope values show a statistically significant separation between upper Bed I paleosol carbonates, modern soil carbonates from the greater Olduvai region, and calcite precipitated under alkaline, evaporative conditions in the center of paleo-Lake Olduvai during Beds I and II. The data indicate a wetter climate during Bed I supported a higher proportion of woody C_3 plants than exist under today's semi-arid climate. Data from Table 2 and references in the text.

from the lake-margin soils exposed in Trench 64 represent the greatest woody C_3 biomass (~ 50 – 60%). The interfluvial and lacustrine $\delta^{13}C$ values are about equally distributed above and below the dataset mean of -4.8‰ . A narrow percentage of C_4 plants (~ 45 – 60% and 45 – 55%) is represented by the interfluvial and Unit B lacustrine facies carbonate $\delta^{13}C$ values.

The carbonate isotopic data were also examined by facies within the stratigraphic units (Fig. 9). For Unit F, the widest range in $\delta^{13}C$ values occurs in the floodplain carbonates (-6.6 to -4.2‰ , averaging -4.6‰ , $n = 11$) and the narrowest in the lake-margin soils (-6.4 to -5.2‰ , averaging -5.8‰ , $n = 4$), with the interfluvial facies intermediate (-5.7 to -4.0‰ , mean of -4.8‰ , $n = 6$). In Unit E the floodplain facies has a wide range of $\delta^{13}C$ values (-5.7 to -3.3‰ , mean of -4.7‰ , $n = 6$); there are only two datapoints each for the interfluvial and lake-margin facies. One sample each was analyzed for the interfluvial and floodplain facies in Unit H. $\delta^{13}C$ values from the lacustrine facies of Unit B were detailed above.

Statistical analyses are appropriate only for Unit F facies; sample sizes for facies groups in Units E and H are too small. Unit F lake-margin $\delta^{13}C$ values are statistically different from floodplain ($P < 0.01$) and interfluvial ($P < 0.05$) data. This finding is consistent with the summary facies data, with woody C_3 vegetation estimated to be slightly more abundant on the lake-margin soils (compare Figs. 8, 9). In Unit F, lake-margin soils, with $\delta^{13}C$ values at or less than -5.2‰ , supported about 40–50% C_4 plants. In contrast, and similar to the summary facies data, the majority (91%, $n = 10$) of valley floodplain $\delta^{13}C$ values for Unit F are greater than the -5.2‰ lake-margin endpoint and represent $>50\%$ C_4 plants. The remaining datapoint for floodplain carbonates within Unit F represents about 40% C_4 biomass. The proportion of C_4 plants supported by the interfluvial facies soils in Unit F ranged from ~ 45 – 60% .

An even more detailed picture might emerge by comparison of specific lithologic units within Bed I. Unfortunately, it is difficult to trace these weakly developed paleosols between trenches, despite their relatively close proximity. We

did, however, sample one calcite horizon within the floodplain facies of Unit F in Trenches 57, 62, and a nearby geologic profile (Table 2). $\delta^{13}C$ values for the calcite average $-4.6 \pm 0.1\text{‰}$ ($n = 3$) and represent $\sim 50\%$ C_4 plants.

A slight temporal difference in paleosol CaCO_3 $\delta^{13}C$ values between Units B, E, and F (Fig. 8) is not significant ($P > 0.05$). Unit H ($n = 2$) was excluded from the statistical tests. $\delta^{13}C$ values range from -5.6 to -4.2‰ (-4.8‰ mean, $n = 7$) in the oldest unit (B), -5.8 to -3.3‰ (-4.9‰ mean, $n = 10$) in Unit E, -6.6 to -4.0‰ (-4.9‰ mean, $n = 21$) in Unit F, and -4.4 and -4.0‰ (-4.2‰ mean, $n = 2$) for the youngest unit (H). Only three datapoints contribute to the slight increase in the range of $\delta^{13}C$ values in Units E and F. The percentages of C_4 biomass represented by the $\delta^{13}C$ values approximate 45–55% for Unit B, 45–60% for Unit E, and 40–55% for Unit F. The two datapoints in Unit H represent $\sim 55\%$ C_4 biomass.

Oxygen isotopes

Analyses of the Bed I oxygen data show significant temporal as well as spatial variation relative to the stratigraphic units and the depositional environments. Evaluation of terrestrial $\delta^{18}O$ values is a qualitative assessment and normally made relative to fluctuations in local or regional pedogenic carbonate data (e.g., Cerling, 1984; Cerling and Hay, 1986; Sikes et al., 1999). Generally, an increase in $\delta^{18}O$ values over time indicates a change in local climatic conditions, from cooler or moister to warmer or drier. $\delta^{18}O$ values of the paleosol carbonates from the Bed I interval range from -5.6 to -3.8‰ , with a mean of -4.7‰ ($n = 40$; Tables 2, 3; Figs. 8, 9). Local soil carbonate $\delta^{18}O$ values have been shown to vary slightly within the same time period, even at approximately the same altitude (Cerling, 1984; Quade et al., 1989b; Marion et al., 1991; Sikes et al., 1999), since soil CaCO_3 is precipitated in soil waters affected by local factors, such as location on the soil catena, or localized evaporation or evapotranspiration associated with differences in density of plant cover.

The differences in $\delta^{18}O$ values between Units B, E, and F (Fig. 8) are statistically significant ($P < 0.05$). Unit H ($n = 2$) was excluded from the statistical evaluation. The range of $\delta^{18}O$ values in the oldest stratigraphic interval, Unit B (-5.5 to -4.3‰ , averaging -4.8‰ , $n = 7$) is followed by comparatively less negative data in Unit E (-5.1 to -3.8‰ , mean of -4.4‰ , $n = 10$). Up sequence, $\delta^{18}O$ values for the periods of CaCO_3 formation in the Unit F paleosols are again lower (-5.6 to -4.2‰ , averaging -4.8‰ , $n = 21$), similar in range to Unit B. Only two samples were analyzed for the youngest interval, Unit H, with $\delta^{18}O$ values of -4.7 and -4.4‰ (-4.5‰ mean).

These data indicate local climatic conditions fluctuated significantly between the time intervals represented by the periods of soil carbonate formation within Units B, E, and F (Fig. 8). Air or soil temperature most likely did not fluctuate much at this equatorial latitude during the relatively short time period under study (Cerling and Quade, 1993). Therefore, we interpret the shift in $\delta^{18}O$ values as a significant change in precipitation, as well as related evaporation rate and plant available water, during the Bed I interval (Table 1, Fig. 8).

The higher $\delta^{18}\text{O}$ values in Unit E suggest it was drier with less precipitation compared to Units B and F. A decrease in $\delta^{18}\text{O}$ values during Unit F suggests precipitation increased. Precipitation may have decreased again after Unit F if the small dataset for the youngest interval is taken as representative.

Differences between paleosol carbonate $\delta^{18}\text{O}$ values for the four depositional environments (Figs. 8, 9) are statistically significant ($P < 0.05$). Difference between the floodplain and interfluvial facies $\delta^{18}\text{O}$ has even greater confidence ($P < 0.01$). This variation in relation to facies is similar to that for the carbon data. Pedogenic carbonates precipitated in the valley floodplain soils have slightly higher $\delta^{18}\text{O}$ values (-5.1 to -3.8‰ , averaging -4.5‰ , $n = 18$) than those from the interfluvial locales outside the valley (-5.6 to -4.3‰ , averaging -5.0‰ , $n = 9$), the lake-margin soils (-4.8 to -4.3‰ , averaging -4.6‰ , $n = 6$), and the oldest unit B (lacustrine facies) soils (-5.5 to -4.3‰ , averaging -4.8‰ , $n = 7$).

There is also a significant difference between the paleosol $\delta^{18}\text{O}$ values recorded within the facies in Unit F ($P < 0.05$). The pattern shown in Figure 9 is similar to the summary facies shown in Figure 8. $\delta^{18}\text{O}$ values are lower within the interfluvial than floodplain and lake-margin depositional environments. Statistical analyses were not appropriate for analyzing facies variation in Units E or H because of the small sample sizes.

When compared to modern soils, the narrow range of variation in carbonate $\delta^{18}\text{O}$ values within each Bed I facies can be considered typical, even though, unlike the recent analogs, more than one period of soil development may be represented. Deviations from mean $\delta^{18}\text{O}$ values have been reported from ± 0.3 to $\pm 2.9\text{‰}$ ($n = 2$ to 5) for recent soil carbonate from a local area at approximately the same altitude (Cerling, 1984; Cerling et al., 1988; Quade et al., 1989b; Marion et al., 1991; Sikes et al., 1999). For Bed I, deviation from the mean is ± 0.5 for interfluvial ($n = 9$), ± 0.3 for floodplain ($n = 18$), ± 0.2 for lake-margin ($n = 6$), and ± 0.4 for lacustrine ($n = 7$) facies carbonates (Table 3). Variation in pedogenic carbonate $\delta^{18}\text{O}$ values from different soils within the Serengeti is comparatively greater ($\pm 0.8\text{‰}$, $n = 6$; Table 2), reflecting differences in vegetation density and the high evaporation rate in today's semi-arid climate. Interestingly, although composite soils are likely represented in Units B, E, and F, deviation from mean $\delta^{18}\text{O}$ values is only $\pm 0.4\text{‰}$ for the carbonates within each of the three units ($n = 7, 10, \text{ and } 21$, respectively).

The pattern in $\delta^{18}\text{O}$ values for the four Bed I facies (Fig. 8) suggests that where the proportion of C_4 grasses was greater, overall plant density may have been lower and, hence, evaporation greater on the floodplains. Alternatively, residence time for soil water may have been shorter on the interfluvial than in the lower valley floodplains or lake margin. $\delta^{18}\text{O}$ values from the interfluvial thus may better approximate paleometeoric water.

Discussion

Paleoenvironment

The paleoenvironmental setting for the western Bed I interval is interpreted as a fluvial plain fringing the western margin

of paleo-Lake Olduvai (Hay, 1976; Hay and Kyser, 2001; Ashley and Hay, 2002). Active volcanism in the Ngorongoro complex periodically ejected pyroclastic material that blanketed the landscape. Major eruptions produced thick beds like Tuff IB (Unit A) or Tuff IC (Unit C) (McHenry, 2004, 2005). Tephra from minor eruptions was added to the land surface and eventually incorporated into the soil (Ashley and Driese, 2000). The prevailing easterly winds would have transported dust to the fluvial plain where it was likely trapped in vegetation within the river valley and baffled by grasses on the interfluvial. Evidence for only one river system was exposed in the excavations (Blumenschine et al., 2003), but there were likely other rivers draining the area surrounding the Olduvai Basin (Hay, 1976).

A wet period is indicated by the expansion of paleo-Lake Olduvai and deposition of the green waxy claystone (Unit B; Table 1). This is followed by a change to drier conditions when the lake shrank, lowering base level and initiating fluvial incision as well as pedogenesis. Although we cannot rule out that hydrological responses of the lake and river were triggered by rift-related tectonics, the stratigraphy of the lake is characterized by periodic lake expansions and contractions (Hay, 1976; Ashley, 2001; Hay and Kyser, 2001). The lake fluctuations are tracked by changes in the paleosol carbonate $\delta^{18}\text{O}$ values, which were precipitated during periods of soil formation (Table 1, Fig. 8). The lake fluctuations are also consistent with regional climate changes interpreted from eolian sediment in marine cores (Fig. 11).

Carbonate-cemented channel sandstones (Unit D) containing mollusks indicate groundwater located in the valley bottom maintained moist conditions for at least part of the year. *Crocodylus* and *Hippopotamus* fossils (Blumenschine et al., 2003) indicate the river was perennial. The lake contracted, the river valley was infilled, and uplands were blanketed with silty tuffaceous claystone (Unit E). The laterally persistent strata, the volcanic composition of the sediment, the development of soils, and the presence of delicate root and insect traces suggest slow, persistent accumulation of airborne dust, which was sourced from the east (Hover and Ashley, 2003; see Fig. 3). A wetter period followed during which the lake expanded onto the fluvial plain, depositing a green waxy claystone (Unit F), exposed at Trench 64 (Fig. 1), succeeded by pedogenesis. The pedogenic carbonate $\delta^{18}\text{O}$ values record this significant shift in climatic conditions. With deposition of Unit H near the top of Bed I, the area returns to a drier period, a finding that concurs with Hay and Kyser (2001).

Based on the paleosol $\delta^{18}\text{O}$ values and comparison to recent soil carbonate data, we suggest annual rainfall during upper Bed I time may have been as high as 800 mm, particularly during the wetter periods recorded in the sediments and paleosol carbonates of Units B and F. $\delta^{18}\text{O}$ values attest that climatic conditions are warmer and much drier in this semi-arid region at present (Table 2; Fig. 10; also see Blumenschine et al., 2003). Today, annual rainfall at Olduvai averages 566 mm and temperature about 23°C (Hay, 1976). Most likely, the $\delta^{18}\text{O}$ values from Bed I result from a dramatic shift in the isotopic composition of meteoric water, possibly coupled with

slightly cooler local air temperature compared to today. Rain-fall during the Bed I interval was probably less than 850 mm since pedogenic carbonate is relatively uncommon where rainfall is >750–850 mm (Cerling, 1984; Cerling and Hay, 1986; Royer, 1999), but moisture was adequate to support the higher proportions of woody C₃ vegetation present during the studied interval in Bed I. Comparison of the -5.0‰ mean for the interfluvial facies (Table 3) with recent soil carbonate $\delta^{18}\text{O}$ values, implies paleometeoric water at Olduvai may have been lower in ^{18}O (-6 to -8‰ SMOW) compared to the present (-1‰ SMOW) (Cerling and Quade, 1993). Today's ^{18}O -enriched water at Olduvai reflects the high rate of preferential evaporation of the lighter isotope (^{16}O) as rain falls through the dry East African atmosphere.

Paleoecology

The series of Olduvai paleolandscapes studied here supported open-canopied grassy woodlands and wooded grasslands, with about 40–60% C₄ grasses, throughout the time interval under study (compare Figs. 4B, 8, 9). This interpretation of the range of $\delta^{13}\text{C}$ values for the Bed I paleosols is based on comparison to modern East African soil datasets and corresponding vegetation communities (Cerling, 1992; Sikes, 1994, 1995). The analog data indicate C₄ biomass may be interpreted as percent grass or percent ground cover since, in these two standard types of vegetational savanna, tropical C₄ grasses dominate the continuous herbaceous layer. None of the carbon data from Bed I correspond to more closed

canopy forest or woodland (with <20% C₄ ground cover), or to open savanna grasslands that typically support >85% C₄ grasses.

To illustrate, modern settings in the East African Rift, with similar proportions of C₄ biomass and the two types of vegetational savanna interpreted from the Bed I $\delta^{13}\text{C}$ values, include the following examples. Wooded grasslands with 70–75% C₄ biomass occur today on portions of the western Lake Naivasha floodplain (central Kenya) and on hilltops overlooking Lake Kwennia in the Ologesailie Basin (southern Kenya). *Acacia xanthophloea* and a mix of *A. mellifera* and *A. tortilis*, respectively, dominate the tree canopy in the two wooded grasslands. Pedogenic carbonate and organic $\delta^{13}\text{C}$ values for the Lake Kwennia soils, for example, are -1.6‰ and -16.0‰ , respectively (Table 2). Grassy woodlands with 50% C₄ ground cover are present on the eastern side of Ngoitokitok Springs in Ngorongoro Crater (northern Tanzania) and near the Makalia River in Lake Nakuru National Park (Central Kenya). *A. xanthophloea* is the dominant tree in these latter two modern analogs.

There is some overlap in interpretation of plant communities from pedogenic carbonate $\delta^{13}\text{C}$ values because of isotopic effects during CaCO₃ formation (e.g., differences in the rate of soil respiration or temperature of carbonate precipitation in different regions). With the theoretical endpoints for soil carbonate $\delta^{13}\text{C}$ values set at -12‰ for 100% C₃ and $+2\text{‰}$ for 100% C₄ terrestrial plants (Cerling, 1992), grassy woodland ranges from about -10 to -2‰ , wooded grassland from about -4.5 to $+1\text{‰}$, and C₄ grassland from about -1 to $+4\text{‰}$.

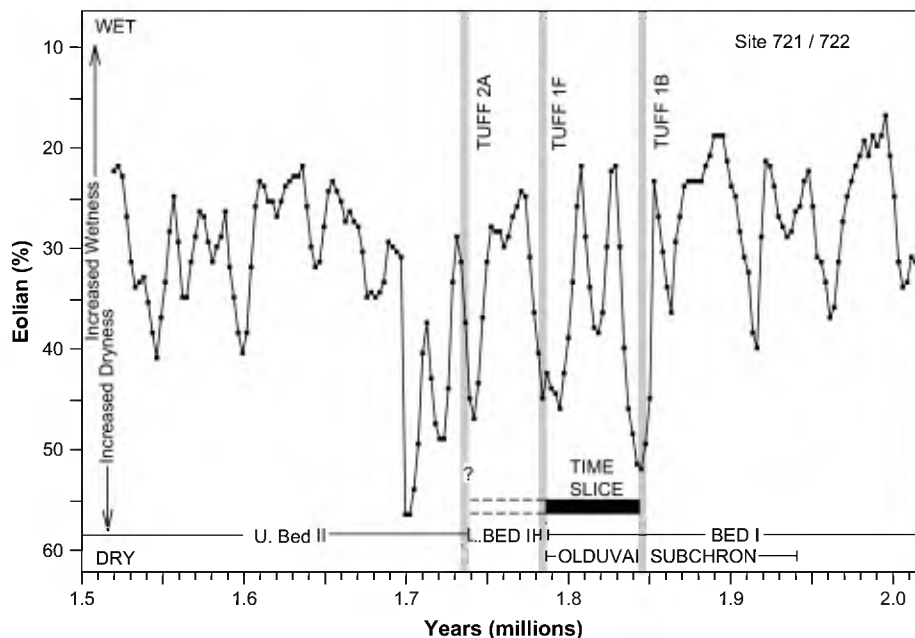


Fig. 11. Data from a marine core (Site 721–722) located 200 km east of Olduvai in the Arabian Sea reveal a rhythmic variation in the percent terrigenous material with time due to the influx of eolian sediment transported from exposed land surfaces (deMenocal and Bloemendal, 1995). Flux increases during dry periods and decreases during wet periods. According to deMenocal and Bloemendal, this fluctuation is related to astronomically driven climatic cycles (Milankovitch cycles). The upper Bed I time-slice lies within the Olduvai paleomagnetic subchron between Tuff IB and Tuff IF. It is in the midst of an overall trend in increasing aridity from 2.0–1.7 Ma. The evidence for short-term climatic fluctuations is consistent with those interpreted in this study. The dashed lines represent excavations by OLAPP into lowermost Bed II. Dates: Tuff IIA estimate from Ashley and Driese (2000); Tuff IF from Hay and Kyser (2001) and McHenry (2005); Tuff IB from Blumenschine et al. (2003).

(Fig. 4B). Though there is spatial variation in the proportion of communities, the majority of Bed I carbonate data (63%, $n = 25$) correspond to a grassy woodland setting, with $\delta^{13}\text{C}$ values between -6.6 and -4.5‰ (Table 2). The remaining paleosol carbonate $\delta^{13}\text{C}$ values (between -4.4 and -3.3‰) may be interpreted as either grassy woodland or wooded grassland. No $\delta^{13}\text{C}$ values from the Bed I carbonates are higher than -3.3‰ .

Interpretation of plant communities using a modern analog scale for soil organic $\delta^{13}\text{C}$ values (Sikes, 1994, 1995) shows similar results. For two co-existing pairs from Units B and E (NS-247-96 and NS-248-96; Table 2), the $\delta^{13}\text{C}$ values of organic carbon and inorganic CaCO_3 correspond to grassy woodland. For two additional pairs (NS-229-96 and NS-245-96), the paleosol organic $\delta^{13}\text{C}$ values correspond to grassy woodland, although the CaCO_3 values (-4.3 and -3.3‰) overlap with the grassy woodland/wooded grassland interface (Fig. 4B). A fifth sample (NS-224-96) with organic carbon data corresponds with riverine forest, but interpretation of this Unit H floodplain sample is problematic because the carbonate-organic spacing (17.9‰) is higher than theoretical, as discussed above. Greater spacing may be related to seasonality (Wang and Follmer, 1998) or to the problem of designating $\delta^{13}\text{C}$ values for the 100% C_3 and C_4 endpoints (see discussion in Sikes, 1999).

The range of $\delta^{13}\text{C}$ values varies significantly between depositional facies but is not significant over time in the Bed I interval. With the exception of the lake-margin facies, the estimated percentages of C_3 and C_4 plants indicate the interfluvial, floodplain, and lacustrine facies (Fig. 8) each supported grassy woodlands and wooded grasslands. The lake-margin facies soils of Trench 64 supported grassy woodlands; this is the only trench for which a geographic pattern for the plant community may be interpreted. Within the stratigraphic units (Fig. 9), vegetation communities within the depositional facies follow a similar pattern to that just described across the Bed I fluvial plain, with grassy woodland to wooded grassland across the Unit E and F time-averaged paleolandscapes on the floodplain soils. For the interfluvial soils, however, the small dataset ($n = 2$) from Unit E is interpreted as grassy woodland while the $\delta^{13}\text{C}$ values from soils developed on the interfluvial deposits of Unit F correspond to grassy woodland and wooded grassland. For Unit H, with just one datapoint each for floodplain and interfluvial soil, the $\delta^{13}\text{C}$ values correspond to grassy woodland and wooded grassland.

Temporal variation in the range of $\delta^{13}\text{C}$ values between Units B, E, and F is relatively minor and not statistically significant. Although the estimated range in the percentage of C_4 plants in Units E and F differ slightly ($\sim 45\text{--}60\%$ in Unit E and $\sim 40\text{--}55\%$ in Unit F), the $\delta^{13}\text{C}$ values correspond to grassy woodland to wooded grassland habitat throughout the sequence shown in Fig. 8.

We hypothesize that the paleowater table throughout the episodes of soil formation may have been slightly higher near Trench 64, closer to the paleolake, since soil moisture is one factor that affects the proportion of trees to grass in modern savanna ecosystems in East Africa (Owen-Smith, 1999). A second factor

influencing the distribution of vegetation communities in a floodplain or lake-margin setting is the relative stability of the environment (Sept, 1994). The woody C_3 vegetation recorded for each of the depositional facies indicates they were relatively stable settings during pedogenic carbonate formation. A third factor affecting savanna types is soil fertility (e.g., Owen-Smith, 1999). Nutrient-rich soils developed on volcanic parent material in Africa today, given sufficient moisture ($\sim 400\text{--}1,000$ mm annual rainfall), typically support savannas dominated by *Acacia* trees. Inadequate or high annual rainfall, on the other hand, may promote savanna grassland, particularly where drainage is impeded on clay-rich substrates or valley floodplains. More well-drained soils are also associated with grassy woodlands and wooded grasslands (Johnson and Tothill, 1984; Belsky, 1990; Owen-Smith, 1999). The fourth factor to consider is time. *Acacia* trees have very rapid growth rates. Young *A. albida*, for example, grow more than one meter a year (Feely, 1965), and *A. xanthophloea* forests are known to develop in only 20 years on the arid, alkaline lakeflats at Amboseli National Park in southern Kenya (Western and van Praet, 1973). Likewise, as predicted by theory (e.g., Berner, 1968; Magaritz et al., 1981) and indicated by other studies of paleosol CaCO_3 (Sikes et al., 1999), the estimated 60,000-year duration of the 6-m section was adequate for the recorded intervals of pedogenesis and related carbonate formation, and complementary recording of fluctuations in vegetation.

These factors, combined with the isotopic data, suggest the vegetation near Trench 64, for example, may have been similar to *Acacia*-dominated groundwater-fed woodlands or grassy woodlands that grow in alkaline lake margins in tropical East Africa today (e.g., Lake Manyara, Tanzania; Lake Nakuru, Kenya). The factors also suggest that soil moisture on the reconstructed lake margin and fluvial plain, in order to support the greater proportion of woody C_3 biomass, was higher than in the Olduvai area at present (see Fig. 10). The vegetation across today's vast Serengeti Plain is mainly comprised of C_4 grasses, *Commiphora* scrub, and *Acacia* trees within a wooded grassland and open C_4 savanna grassland mosaic with $\sim 80\text{--}100\%$ C_4 plants. In contrast, a mosaic of grassy woodlands and wooded grasslands, with only $\sim 40\text{--}60\%$ C_4 plants, is reconstructed for the series of Bed I paleolandscapes. In further support of wetter periods and the presence of trees on the early Pleistocene landscape at Olduvai is fossil wood collected in the lowermost Bed II eastern lake margin by the OLAPP team (Bamford, 2005). Dating to approximately 1.8–1.75 Ma, the wood from HWK-East is identified as *Guibourtia coleosperma*, a large, shade tree that grows up to 19-m high. A member of the Sudano-Zambesian phytochorion (Werger and Coetzee, 1978) and the Caesalpinaceae family, this species occurs today in mixed woodland south of Tanzania.

Paleoclimate

There is a growing body of literature suggesting wet/dry cycles occur in the East African Rift in concert with astronomically driven (Milankovitch) glacial-interglacial obliquity

cycles (~41,000 yrs) in addition to precession cycles (19,000–23,000 yrs; Pokras and Mix, 1987; Gasse et al., 1989; Ruddiman et al., 1989; Imbrie et al., 1993; deMenocal and Bloemendal, 1995; Trauth et al., 2005; Deino et al., 2006). Although the continental record is discontinuous and cannot be expected to mirror the marine sedimentary sequence (see Sikes, 1999), stable isotopic studies of paleosols have been correlated with other continental or global proxy records of paleoclimate (Smith et al., 1993; deMenocal, 1995; Quade et al., 1995). Further, lacustrine ecosystems like paleo-Olduvai are most appropriate for such studies because small, closed basins are highly sensitive to climatic fluctuations (e.g., Feibel, 1999).

Analysis of eolian dust in marine cores for the time period of this study shows that dust fluctuated by 25% over the 60-kyr interval with ~20-kyr periodicity (deMenocal and Bloemendal, 1995). Climate change is typical throughout the Plio-Pleistocene (Fig. 11) and climate stasis for long periods of time is very unlikely. Both the lithologic and stable isotopic record in western Bed I appear to reflect the continually changing climatic conditions in the environment (Table 1, Fig. 8). Based on an estimated sedimentation rate of 1 m/10,000 years (Ashley and Driese, 2000), the isotope values would likely be time-averaged over several hundreds or thousands of years for soil formation. It appears that despite time averaging, climatic fluctuations were faithfully recorded in the pedogenic carbonates in response to the changing depositional environments.

Other Bed I research

The results obtained here agree well with previous isotopic research reported on paleosol carbonates from Bed I (Cerling et al., 1977; Cerling and Hay, 1986; also see Cerling, 1992). $\delta^{13}\text{C}$ values ranging from -5 to -4.2‰ for three pedogenic carbonates from the western lake margin suggest the presence of a grassy woodland below Tuff IA just above the basal lava (Hay, R.L., pers. comm. on sample locations). Four pedogenic carbonates have been previously analyzed from the eastern lake margin between Tuffs IB and IF. The lowermost is from the FLK (level 22) *Zinjanthropus* paleosol between Tuffs IB and IC, for which grassy woodland has been reconstructed (Sikes, 1994). Grassy woodland is also indicated by a $\delta^{13}\text{C}$ value (-5.8‰) for CaCO_3 sampled about a meter below Tuff IF, and grassy woodland/wooded grassland for samples collected within 30 cm of Tuff IF (-3.8‰ , $n = 2$). $\delta^{18}\text{O}$ values (-5.5‰ , $n = 3$) for the western lake-margin carbonates are comparable to those reported here, while the range for eastern lake-margin $\delta^{18}\text{O}$ values (-6.5 to -5.3‰ , $n = 4$) is slightly lower. The proximity of the eastern lake-margin samples, obtained from localities 85 and 45, to the groundwater-fed wetland (Fig. 3) may account for this difference, as recently interpreted for carbonate rhizoliths sampled from the wetlands (Liutkus et al., 2005).

As noted, a small subset ($n = 7$) of the isotopic data reported here provided a general environmental background for western Bed I in the OLAPP publication on the discovery

of OH 65 (Blumenschine et al., 2003). The subset, between Tuffs IB and IC, corresponds to Unit B of the present study, reconstructed with a grassy woodland and wooded grassland mosaic. Most likely the Unit B paleosol carbonates were precipitated prior to the channel incision in which the hominin assemblage was found. Based on modern analogs and faunal evidence, Blumenschine and others suggest gallery woodland may also have been present along the riverbank. $\delta^{13}\text{C}$ values from tooth enamel confirm the presence of C_4 grasses within the habitat range of several grazing species within the time frame reported for OH 65 between Tuff IB and the top of the Olduvai Subchron.

Direct comparison can be made between our results on the western side of paleo-Lake Olduvai with paleoecological interpretations from sites excavated on its eastern margin (Leakey, 1971) for the period between Tuff IB and Tuff IC. Between Tuff IC and Tuff IF, however, a comparison of paleoecology cannot be made between the two sides of the lake without more precise age constraints (see Fig. 2). Nonetheless, the present study is in broad agreement with reconstructions based on the excavated large and small mammal assemblages, which conclude that a higher proportion of intermediate and closed habitats were present during Bed I than in the area today (Plummer and Bishop, 1994; Kappelman et al., 1997; Fernández-Jalvo et al., 1998; Andrews and Humphrey, 1999; Bishop, 1999; Denys, 1999; Plummer et al., 1999). Between Tuffs IB and IC, interpretations of site-specific data from FLK-NN (levels 1, 2, and 3) and FLK-*Zinjanthropus* indicate the presence of dense canopy woodland based on the micro-mammal assemblages (Fernández-Jalvo et al., 1998; Andrews and Humphrey, 1999) and closed habitats based on bovid ecomorphology (Plummer and Bishop, 1994). By implication, these data indicate the climate during portions of Bed I time was moister than today. Further, fossil pollen spectra from lower Bed I (just below Tuff IB) indicate tree cover in the paleobasin was denser and suggest rainfall approached 800–900 mm (Bonnefille and Riollet, 1980).

Landscape-scale research

This study of a Plio-Pleistocene “time-slice” in Olduvai Gorge provides an example of a series of reconstructed paleolandscapes that are rich in detail and add a small piece to the puzzle of the environmental context in which hominins evolved. This type of landscape-scale research is another step toward an understanding of the complex relationship between hominin behavior and ecology. The effective use of geologic basins as ecosystems provides us with the bridge needed to connect local physical or biological events witnessed in the discontinuous terrestrial record to climatic perturbations documented in the global record (Feibel, 1999). A comparison of landscape-scale research between basins and within basins over time is likewise essential to determination of cause and effect (Potts, 1994; Potts et al., 1999), and must be achieved before we can decide between conflicting scenarios that seek to answer how vegetation and climate affected human evolution. After this information is generated, we can evaluate the

data and test, for example, whether savanna grassland expansion (Bartholomew and Birdsell, 1953; Wolpoff, 1980), a “turn-over pulse” associated recently with global records of steplike cooling and drying (Vrba et al., 1989, 1995; deMenocal, 1995), or a widening range of environmental variation (Potts, 1996, 1998) most influenced hominin evolution and adaptive changes.

Conclusions

Paleolandscape research at Olduvai Gorge has documented the presence of a river system in the western exposures of upper Bed I above Tuff IB. A fluvial plain developed on a surface comprised of quartzofeldspathic sediments eroded from shallow basement rocks, airborne pyroclastic material transported directly from erupting volcanoes, and eolian sediment reworked from lake-margin flats (Ashley and Hay, 2002). Rivers drained eastward from the Serengeti Plain into a small lake that periodically expanded onto the fluvial plain. The lithologic record indicates a moist period (lake and fluvial deposits) was followed by drier conditions (eolian and soil forming processes), with a return to slightly moister conditions (minor lake expansion) and another drier period near the top of Bed I. The deposits date between ~ 1.845 – 1.785 Ma and lie within the Olduvai Subchron (Hay and Kyser, 2001; Blumenschine et al., 2003; McHenry, 2005).

During this $\sim 60,000$ -year segment of sedimentation and soil formation, oxygen isotopic results from paleosol carbonates vary significantly over time, recording increases and decreases in local precipitation. These shifts support the climatic conditions interpreted from the western Bed I lithologic record and regional climate interpreted from marine cores (deMenocal and Bloemendal, 1995). Throughout the sequence, $\delta^{13}\text{C}$ values from paleosol carbonates and organic matter record differing percentages of C_4 grasses, ranging between ~ 40 – 60% , and variable proportions of grassy woodland to wooded grassland. In contrast to today’s savanna grassland mosaic on the semi-arid Serengeti Plain, higher annual rainfall provided adequate moisture for the comparatively higher proportions of woody C_3 vegetation. Both the lithological and stable isotope record in western Bed I appear to reflect the changing conditions recorded in global proxies of paleoclimate during this period.

Acknowledgements

The data on which this paper is based were collected between 1995 and 1999 under permits issued to R.J. Blumenschine and F.T. Masao by the Tanzania Commission for Science and Technology and the Tanzania Department of Antiquities, to whom we are grateful. We thank D.M. Deocampo, C.C. Swisher III, A.L. Deino, and G.F. Mollel for discussions on the geology; A.E. Cushing, S.R. Copeland, J.C. Tactikos, J.K. Njau, R. Mrema, J. Temba, G. Peter, and A. Venance for excavation of the western Bed I trenches; J.I. Ebert and J. Paiva for the GPS readings used to locate the trenches; and J.S. Delaney for drafting. We are particularly grateful to Richard Hay for his valuable insights into the stratigraphy of Olduvai and his generosity in

discussing ideas and sharing data. R. Potts, J. Quade, and four anonymous reviewers provided suggestions and comments that improved the manuscript. Field or laboratory research for OLAPP was sponsored by numerous grants: National Science Foundation (Geosciences 9903258 to Ashley; Archaeology SBR-9805846 to Sikes; SBR-9602478, SBR-9601065, BNS-9000099 to Blumenschine and Masao); L.S.B. Leakey Foundation (Sikes; Blumenschine and Masao); Wenner-Gren Foundation (Blumenschine and Masao); Rutgers University (Blumenschine); National Geographic Society (Ebert); Boise Fund (Sikes); and Human Origins and Scholarly Studies Programs, Smithsonian Institution (Sikes). This manuscript was prepared by Sikes while a member of the Human Origins Program, National Museum of Natural History. Isotope analyses (preparation and gas collection) were performed by Sikes in the Smithsonian Light Isotope Laboratory at the Smithsonian.

References

- Alam, M.S., Keppens, E., Paepe, R., 1997. The use of oxygen and carbon isotope composition of pedogenic carbonates from Pleistocene palaeosols in NW Bangladesh, as palaeoclimatic indicators. *Quatern. Sci. Rev.* 16, 161–168.
- Ambrose, S.H., Sikes, N.E., 1991. Soil organic carbon isotopic evidence for vegetation change in the Kenya Rift Valley. *Science* 253, 1402–1405.
- Andrews, P., Humphrey, L., 1999. African Miocene environments and the transition to early hominines. In: Bromage, T.G., Schrenk, F. (Eds.), *African Biogeography, Climate Change, and Human Evolution*. Oxford University Press, Oxford, pp. 282–300.
- Ashley, G.M., 2001. Orbital rhythms, monsoons, and playa lake response, Olduvai basin, equatorial East Africa at 1.85–1.75 Ma. *Eos Trans. Am. Geophys. Union* 82 (47), F759.
- Ashley, G.M., Driese, S.G., 2000. Paleopedology and paleohydrology of a volcanoclastic paleosol: implications for Early Pleistocene paleoclimate record, Olduvai Gorge, Tanzania. *J. Sediment. Res.* 70, 1065–1080.
- Ashley, G.M., Hay, R.L., 2002. Sedimentation patterns in a Plio-Pleistocene volcanoclastic rift-margin basin, Olduvai Gorge, Tanzania. In: Renault, R.W., Ashley, G.M. (Eds.), *Sedimentation in Continental Rifts*. SEPM Special Publication, 73, pp. 107–122.
- Bamford, M.K., 2005. Early Pleistocene fossil wood from Olduvai Gorge, Tanzania. *Quatern. Int.* 129, 15–22, doi:10.1016/j.quaint.2004.04.003.
- Bartholomew Jr., G.A., Birdsell, J.B., 1953. Ecology and the protohominids. *Am. Anthropol.* 55, 481–498.
- Belsky, A.J., 1990. Tree-grass ratios in East African savannas: a comparison of existing models. *J. Biogeogr.* 17, 483–489.
- Berner, R.N., 1968. Rate of concretion growth. *Geochim. Cosmochim. Acta* 32, 477–483.
- Birkeland, P.W., 1984. *Soils and Geomorphology*. Oxford University Press, New York.
- Bishop, L.C., 1999. Suid paleoecology and habitat preferences at African Pliocene and Pleistocene hominid localities. In: Bromage, T.G., Schrenk, F. (Eds.), *African Biogeography, Climate Change, and Human Evolution*. Oxford University Press, Oxford, pp. 216–225.
- Blodgett, R.H., 1988. Calcareous paleosols in the Triassic Dolores Formation, southwestern Colorado. In: Reinhardt, J., Sigleo, W.R. (Eds.), *Paleosols and Weathering Through Geologic Time: Principles and Applications*. *Geol. Soc. Am. Spec. Pap.* 216, 103–120.
- Blumenschine, R.J., Masao, F.T., 1991. Living sites at Olduvai Gorge, Tanzania? Preliminary landscape archaeology results in the basal Bed II lake margin zone. *J. Hum. Evol.* 21, 451–462.
- Blumenschine, R.J., Masao, F.T., Ashley, G.M., Clarke, R.J., Ebert, J.I., Peters, C.R., Sikes, N.E., van der Merwe, N.J., 1997. New paleoanthropological discoveries and tests of hominid land use models in the western

- lacustrine plain of the lowermost Bed II Olduvai Basin. *J. Hum. Evol.* 32, A5, doi:10.1006/jhev.1996.0131.
- Blumenschine, R.J., Peters, C.R., Masao, F.T., Ashley, G.M., Ebert, J.I., 1999. Preliminary tests of paleoanthropological predictions for hominid land use in the east-central portion of the lowermost Bed II Olduvai Basin, Tanzania. *J. Hum. Evol.* 36, A2–A3. doi:10.1006/jhev.1999.0293.
- Blumenschine, R.J., Peters, C.R., Masao, F.T., Clarke, R.J., Deino, A.L., Hay, R.L., Swisher III, C.C., Stanistreet, I.G., Ashley, G.M., McHenry, L.J., Sikes, N.E., van der Merwe, N.J., Tactikos, J.C., Cushing, A.E., Deocampo, D.M., Njau, J.K., Ebert, J.I., 2003. Late Pliocene Homo and hominid land use from western Olduvai Gorge, Tanzania. *Science* 299, 1217–1221; Supporting online material at: www.sciencemag.org/cgi/content/full/299/5610/1217/DC1.
- Bonnefille, R., Riollet, G., 1980. Palynologie, végétation et climats de Bed I et Bed II à Olduvai, Tanzanie. In: Leakey, R.E., Ogot, B.A. (Eds.), *Proceedings of the Eighth Pan-African Congress of Prehistory & Quaternary Studies*. The International Louis Leakey Memorial Institute for African Prehistory, Nairobi, pp. 123–127.
- Bonnefille, R., Roeland, J.C., Guiot, J., 1990. Temperature and rainfall estimates for the past 40,000 years in equatorial Africa. *Nature* 346, 347–349.
- Bown, T.M., Beard, K.C., 1990. Systematic lateral variation in the distribution of fossil mammals in alluvial paleosols, lower Eocene Willwood Formation, Wyoming. *Geol. Soc. Am. Spec. Pap.* 243, 35–151.
- Bridge, J.S., 2003. *Rivers and Floodplains*. Blackwell Science Ltd, Oxford.
- Cerling, T.E., 1984. The stable isotopic composition of modern soil carbonate and its relationship to climate. *Earth Planet. Sci. Lett.* 71, 229–240.
- Cerling, T.E., 1992. Development of grasslands and savannas in East Africa during the Neogene. *Palaeogeogr. Palaeoclimat. Palaeoecol.* 97, 241–247.
- Cerling, T.E., Bowman, J.R., O'Neil, J.R., 1988. An isotopic study of a fluvial-lacustrine sequence: the Plio-Pleistocene Koobi Fora sequence, East Africa. *Palaeogeogr. Palaeoclimat. Palaeoecol.* 63, 335–356.
- Cerling, T.E., Ehleringer, J.R., Harris, J.M., 1998. Carbon dioxide starvation, the development of C₄ ecosystems, and mammalian evolution. *Phil. Trans. R. Soc. Lond. B* 353, 159–171.
- Cerling, T.E., Harris, J.M., MacFadden, B.J., Leakey, M.G., Quade, J., Eisenmann, V., Ehleringer, J.R., 1997. Global vegetation change through the Miocene/Pliocene boundary. *Nature* 389, 153–158.
- Cerling, T.E., Hay, R.L., 1986. An isotopic study of paleosol carbonates from Olduvai Gorge. *Quatern. Res.* 25, 63–78.
- Cerling, T.E., Hay, R.L., O'Neil, J.R., 1977. Isotopic evidence for dramatic climatic changes in East Africa during the Pleistocene. *Nature* 267, 137–138.
- Cerling, T.E., Quade, J., 1993. Stable carbon and oxygen isotopes in soil carbonates. In: Swart, P.K., Lohmann, K.C., McKenzie, J., Savin, S. (Eds.), *Climate Change in Continental Isotopic Records*. Geophysical Monograph 78, pp. 217–231.
- Cerling, T.E., Quade, J., Ambrose, S.H., Sikes, N.E., 1991. Miocene fossil soils, grasses and carbon isotopes from Fort Ternan (Kenya): grassland or woodland? *J. Hum. Evol.* 21, 295–306.
- Cerling, T.E., Quade, J., Wang, Y., Bowman, J.R., 1989. Carbon isotopes in soils and paleosols as ecology and paleoecology indicators. *Nature* 341, 138–139.
- Cole, M.M., 1963. Vegetation nomenclature and classification with particular reference to the savannas. *South Afr. Geogr. J.* 55, 3–14.
- Deines, P., 1980. The isotopic composition of reduced organic carbon. In: Fritz, P., Fontes, J.C. (Eds.), *Handbook of Environmental Isotope Geochemistry*. The Terrestrial Environment, vol. 1. A. Elsevier, Amsterdam, pp. 329–406.
- deMenocal, P.B., 1995. Plio-Pleistocene African climate. *Science* 270, 53–59.
- deMenocal, P.B., Bloemendal, J., 1995. Plio-Pleistocene climatic variability in subtropical Africa and the paleoenvironment of hominid evolution: a combined data-model approach. In: Vrba, E.S., Denton, G.H., Partridge, T.C., Burkle, L.H. (Eds.), *Paleoclimate and Evolution with Emphasis on Human Origins*. Yale University Press, New Haven, pp. 262–288.
- Deino, A.L., Kingston, J.D., Glen, J.M., Edgar, R.K., Hill, A., 2006. Precessional forcing of lacustrine sedimentation in the late Cenozoic Chemeron Basin, Central Kenya Rift, and calibration of Gauss/Matuyama boundary. *Earth Planet. Sci. Lett.* 247, 41–60.
- Denys, C., 1999. Of mice and men: evolution in East and South Africa during Plio-Pleistocene times. In: Bromage, T.G., Schrenk, F. (Eds.), *African Biogeography, Climate Change, and Human Evolution*. Oxford University Press, Oxford, pp. 226–252.
- Feely, J.M., 1965. Observations on *Acacia albida* in the Luangwa Valley. *Puku* 3, 67–70.
- Feibel, C., 1999. Basin evolution, sedimentary dynamics, and hominid habitats in East Africa. In: Bromage, T.G., Schrenk, F. (Eds.), *African Biogeography, Climate Change, and Human Evolution*. Oxford University Press, Oxford, pp. 276–281.
- Fernández-Jalvo, Y., Denys, C., Andrews, P., Williams, T., Dauphin, Y., Humphrey, L., 1998. Taphonomy and palaeoecology of Olduvai Bed-I (Pleistocene, Tanzania). *J. Hum. Evol.* 34, 137–172. doi:10.1006/jhev.1997.0188.
- Freytet, P., Plaziat, J.C., 1982. Continental carbonate sedimentation and pedogenesis—Late Cretaceous and Early Tertiary of southern France. *Contrib. Sedimentol.* 12, 1–213.
- Friedli, H., Lotscher, H., Oeschger, H., Siegenthaler, U., Stauffer, B., 1986. Ice core record of the ¹³C/¹²C ratio of atmospheric CO₂ in the past two centuries. *Nature* 324, 237–238.
- Gasse, F., Lédée, V., Massault, M., Fontes, F.C., 1989. Water level fluctuations of Lake Tanganyika in phase with oceanic changes during the last glaciation and deglaciation. *Nature* 342, 57–59.
- Gile, L.H., Peterson, F.F., Grossman, R.B., 1966. Morphological and genetic sequences of carbonate accumulation in desert soils. *Soil Sci.* 101 (5), 347–360.
- Goudie, A., 1973. *Duricrusts in Tropical and Subtropical Landscapes*. Clarendon Press, Oxford.
- Grommé, C.S., Hay, R.L., 1971. Geomagnetic polarity epochs: age and duration of the Olduvai normal polarity event. *Earth Planet. Sci. Lett.* 10, 179–185.
- Hay, R.L., 1976. *Geology of the Olduvai Gorge*. University of California Press, Berkeley.
- Hay, R.L., 1987. *Geology of the Laetoli area*. In: Leakey, M.D., Harris, J.M. (Eds.), *Laetoli: a Pliocene Site in Northern Tanzania*. Clarendon Press, Oxford, pp. 23–47.
- Hay, R.L., 1989. Holocene carbonatite-nephelinite tephra deposits of Oldoinyo Lengai, Tanzania. *J. Volcanol. Geotherm. Res.* 37, 77–91.
- Hay, R.L., Kyser, T.K., 2001. Chemical sedimentology and paleoenvironmental history of Lake Olduvai, a Pleistocene lake in northern Tanzania. *Geol. Soc. Am. Bull.* 113, 1505–1521.
- Hover, V.C., Ashley, G.M., 2003. Geochemical signatures of paleodepositional and diagenetic environments: a STEM/AEM study of authigenic clay minerals from an arid rift basin, Olduvai Gorge, Tanzania. *Clay Clay Miner.* 51, 231–251.
- Imbrie, J., Berger, A., Shackleton, N.J., 1993. Role of orbital forcing: a two-million-year perspective. In: Eddy, J.A., Oeschger, H. (Eds.), *Global Changes and the Perspective of the Past*. John Wiley & Sons, London, pp. 263–277.
- Isaac, G.L., Harris, J.W.K., 1980. A method for determining the characteristics of artifacts between sites in the Upper Member of the Koobi Fora Formation, East Lake Turkana. In: Leakey, R.E., Ogot, B.A. (Eds.), *Proceedings of the Eighth Pan-African Congress of Prehistory & Quaternary Studies*. The International Louis Leakey Memorial Institute for African Prehistory, Nairobi, pp. 19–22.
- Isaac, G.L., Harris, J.W.K., 1997. The stone artefact assemblage: a comparative study. In: Isaac, G.L. (Ed.), *Plio-Pleistocene Archaeology*. Koobi Fora Research Project, vol. 5. Clarendon Press, Oxford, pp. 262–362.
- Jenny, H., 1980. *The Soil Resource*. Springer-Verlag, New York.
- Johnson, R.W., Tohill, J.C., 1984. Definition and broad geographic outline of savanna lands. In: Tohill, J.C., Mott, J.J. (Eds.), *Ecology and Management of the World's Savannas*. Australian Academy of Science, Canberra, pp. 1–13.
- Kappelman, J., Plummer, T., Bishop, L., Duncan, A., Appleton, S., 1997. Bovids as indicators of Plio-Pleistocene paleoenvironments in East Africa. *J. Hum. Evol.* 32, 229–256. doi:10.1006/jhev.1996.0105.
- Kingston, J.D., Marino, B.D., Hill, A., 1994. Isotopic evidence for Neogene hominid paleoenvironments in the Kenya Rift Valley. *Science* 264, 955–959.
- Klappa, C.F., 1980. Rhizoliths in terrestrial carbonates: classification, recognition, genesis and significance. *Sedimentology* 27, 613–629.

- Leakey, M.D., 1971. Olduvai Gorge. In: *Excavations in Beds I and II, 1960–1963*, vol. 3. Cambridge University Press, Cambridge.
- Livingstone, D.A., Clayton, W.D., 1980. An altitudinal cline in African tropical grass floras and its paleoecological significance. *Quatern. Res.* 13, 382–402.
- Lourens, L.J., Antonarakou, A., Hilgen, F.J., van Hoof, A.A.M., Vergnaud-Grazzini, C., Zachariasse, W.J., 1996. Evaluation of the Plio-Pleistocene astronomical timescale. *Paleoceanography* 11, 391–413.
- Liutkus, C.M., Ashley, G.M., 2003. Facies model of a semi-arid freshwater wetland, Olduvai Gorge, Tanzania. *J. Sediment. Res.* 73, 691–795.
- Liutkus, C.M., Wright, J.D., Ashley, G.M., Sikes, N.E., 2005. Paleoenvironmental interpretation of lake-margin deposits using $\delta^{13}\text{C}$ and $\delta^{18}\text{O}$ results from Early Pleistocene carbonate rhizoliths, Olduvai Gorge, Tanzania. *Geology* 33, 377–380.
- Machette, M.N., 1985. Calcic soils of the southwestern United States. In: Weide, D.L. (Ed.), *Soils and Quaternary Geology of the Southwestern United States*. Geol. Soc. Am. Spec. Pap. No. 203, 1–21.
- Magaritz, M., Kaufman, A., Yaalon, D.H., 1981. Calcium carbonate nodules in soils: $^{18}\text{O}/^{16}\text{O}$ and $^{13}\text{C}/^{12}\text{C}$ ratios and ^{14}C contents. *Geoderma* 25, 157–172.
- Marion, G.M., Introne, D.S., VanCleve, K., 1991. The stable isotope geochemistry of CaCO_3 on the Tanana River floodplain of interior Alaska, U.S.A.: composition and mechanisms of formation. *Chem. Geol. (Isot. Geosci. Sect.)* 86, 97–110.
- McHenry, L.J., 2004. Characterization and correlation of altered Plio-Pleistocene tephra using a “multiple technique” approach: case study at Olduvai Gorge, Tanzania. Ph.D. Dissertation, Rutgers University.
- McHenry, L.J., 2005. Phenocryst composition as a tool for correlating fresh and altered tephra, Bed I, Olduvai Gorge, Tanzania. *Stratigraphy* 2, 101–115.
- Morgan, M.E., Kingston, J.D., Marino, B.D., 1994. Carbon isotopic evidence for the emergence of C_4 plants in the Neogene from Pakistan and Kenya. *Nature* 367, 162–165.
- Owen-Smith, N., 1999. Ecological links between African savanna environments, climate change, and early hominid evolution. In: Bromage, T.G., Schrenk, F. (Eds.), *African Biogeography, Climate Change, and Human Evolution*. Oxford University Press, Oxford, pp. 138–149.
- Plummer, T.W., Bishop, L.C., 1994. Hominid paleoecology as indicated by antelope remains. *J. Hum. Evol.* 24, 47–75, doi:10.1006/jhev.1994.1035.
- Plummer, T., Bishop, L., Kingston, J., Sikes, N., Ditchfield, P., Hertel, F., Ferraro, J., 1999. Reconstructing Oldowan hominid paleoecology. *J. Hum. Evol.* 36, A18, doi:10.1006/jhev.1999.0293.
- Pokras, E.M., Mix, A.C., 1987. Earth’s precession cycle and Quaternary climatic change in tropical Africa. *Nature* 326, 486–487.
- Potts, R., 1989. Olorgesailie: new excavations and findings in Early and Middle Pleistocene contexts, southern Kenya rift valley. *J. Hum. Evol.* 18, 477–484.
- Potts, R., 1994. Variables versus models of early Pleistocene hominid land use. *J. Hum. Evol.* 27, 7–24, doi:10.1006/jhev.1994.1033.
- Potts, R., 1996. Evolution and climate variability. *Science* 273, 922–923.
- Potts, R., 1998. Environmental hypotheses of hominin evolution. *Yearb. Phys. Anthropol.* 41, 93–136.
- Potts, R., Behrensmeier, A.K., Ditchfield, P., 1999. Paleolandscapes variation and Early Pleistocene hominid activities: members I and 7, Olorgesailie Formation, Kenya. *J. Hum. Evol.* 37, 747–788, doi:10.1006/jhev.1999.0344.
- Pratt, D.J., Greenway, P.J., Gwynne, M.D., 1966. A classification of East African rangeland, with an appendix on terminology. *J. Appl. Ecol.* 3, 369–382.
- Pratt, D.J., Gwynne, M.D. (Eds.), 1977. *Rangeland Management and Ecology in East Africa*. Krieger, Huntington.
- Quade, J., Cater, J.M.L., Ojha, T.P., Adam, J., Harrison, T.M., 1995. Late Miocene environmental change in Nepal and the northern Indian subcontinent: stable isotopic evidence from paleosols. *Geol. Soc. Am. Bull.* 107 (12), 1381–1397.
- Quade, J., Cerling, T.E., Bowman, J.R., 1989a. Development of Asian monsoon revealed by marked ecological shift during the latest Miocene in northern Pakistan. *Nature* 342, 161–166.
- Quade, J., Cerling, T.E., Bowman, J.R., 1989b. Systematic variations in the carbon and oxygen isotopic composition of pedogenic carbonate along elevation transects in the southern Great Basin, United States. *Geol. Soc. Am. Bull.* 101, 464–475.
- Quade, J., Roe, L.J., 1999. The stable-isotope composition of early groundwater cements from sandstone in paleoecological reconstruction. *J. Sediment. Res.* 69, 667–674.
- Retallack, G.J., 1990. *Soils of the Past: an Introduction to Paleopedology*. Unwin Hyman, London.
- Royer, D.L., 1999. Depth to pedogenic carbonate horizon as a paleoprecipitation indicator? *Geology* 27, 1123–1126.
- Ruddiman, W.F., Sarnthein, M., Baldauf, J., Backman, J., Curry, W., Dupont, L.M., Janecek, T., Pokras, E.M., Raymo, M.E., Stabell, B., Stein, R., Tiedemann, R., 1989. Late Miocene to Pleistocene evolution of climate in Africa and the low-latitude Atlantic: overview of leg 108 results. In: Ruddiman, W., Sarnthein, M. (Eds.), *Proceedings of Ocean Drilling Program*, vol. 108. Ocean Drilling Program, College Station, pp. 463–484.
- Sept, J.M., 1994. Beyond bones: archaeological sites, early hominid subsistence, and the costs and benefits of exploiting wild plant foods in east African riverine landscapes. *J. Hum. Evol.* 27, 295–320, doi:10.1006/jhev.1994.1047.
- Sikes, N.E., 1994. Early hominid habitat preferences in East Africa: paleosol carbon isotopic evidence. *J. Hum. Evol.* 27, 25–45, doi:10.1006/jhev.1994.1034.
- Sikes, N.E., 1995. Early hominid habitat preferences in East Africa: stable isotopic evidence from paleosols. Ph.D. Dissertation, University of Illinois-Urbana.
- Sikes, N.E., 1996. Hominid habitat preferences in lower Bed II: stable isotope evidence from paleosols. *Kaupia* 6, 231–238. First presented at: “Four Million Years of Hominid Evolution in Africa: an International Congress in Honour of Dr. Mary D. Leakey’s Outstanding Contribution in Palaeoanthropology” Arusha, Tanzania, August 1993.
- Sikes, N.E., 1999. Plio-Pleistocene floral context and habitat preferences of sympatric hominid species in East Africa. In: Bromage, T.G., Schrenk, F. (Eds.), *African Biogeography, Climate Change, and Human Evolution*. Oxford University Press, Oxford, pp. 301–315.
- Sikes, N.E., 2000. Using paleosol stable isotopes to reconstruct Olduvai basin landscapes. *J. Hum. Evol.* 38, A28, doi:10.1006/jhev.1999.0393.
- Sikes, N.E., Potts, R., Behrensmeier, A.K., 1997. Isotopic study of Pleistocene paleosols from the Olorgesailie Formation, southern Kenya rift. *J. Hum. Evol.* 32, A20–A21, doi:10.1006/jhev.1996.0131.
- Sikes, N.E., Potts, R., Behrensmeier, A.K., 1999. Early Pleistocene habitat in Member I Olorgesailie based on paleosol stable isotopes. *J. Hum. Evol.* 37, 721–746, doi:10.1006/jhev.1999.0343.
- Slate, J.L., Smith, G.A., Wang, Y., Cerling, T.E., 1996. Carbonate-paleosol genesis in the Plio-Pleistocene St. David Formation, southeastern Arizona. *J. Sediment. Res.* 66, 85–94.
- Smith, G.A., Wang, Y., Cerling, T.E., Geissman, J.W., 1993. Comparison of a paleosol-carbonate isotope record to other records of Pliocene-early Pleistocene climate in the western United States. *Geology* 21, 691–694.
- Stern, N., 1993. The structure of the lower Pleistocene archaeological record: a case study from the Koobi Fora Formation. *Curr. Anthropol.* 34 (3), 201–225.
- Tamrat, E., Thouveny, N., Taieb, M., Opdyke, N.D., 1995. Revised magnetostratigraphy of the Plio-Pleistocene sedimentary sequence of the Olduvai Formation (Tanzania). *Palaeogeogr. Palaeoclimat. Palaeoecol.* 114, 273–283.
- Taylor, D.M., 1992. Pollen evidence from Muchoya Swamp, Rukiga Highlands (Uganda), for abrupt changes in vegetation during the last ca. 21,000 years. *Bull. Soc. Géol. Fr.* 1, 77–82.
- Tieszen, L.L., Senyimba, M.M., Imbamba, S.K., Troughton, J.H., 1979. The distribution of C_3 and C_4 grasses along an altitudinal and moisture gradient in Kenya. *Oecologia* 37, 337–350.
- Trauth, M.H., Maslin, M.A., Deino, A., Strecker, M.R., 2005. Late Cenozoic moisture history of East Africa. *Science* 309, 2051–2053.
- Vrba, E.S., Denton, G.H., Partridge, T.C., Burkle, L.H. (Eds.), 1995. *Paleoclimate and Evolution with Emphasis on Human Origins*. Yale University Press, New Haven.
- Vrba, E.S., Denton, G.H., Prentice, M.L., 1989. Climatic influences on early hominid behavior. *Ossa* 14, 127–156.
- Walter, R.C., Manega, P.C., Hay, R.L., Drake, R.E., Curtis, G.H., 1991. $^{40}\text{Ar}/^{39}\text{Ar}$ dating of Bed I, Olduvai Gorge, Tanzania. *Nature* 354, 145–149.

- Wang, H., Follmer, L.R., 1998. Proxy of monsoon seasonality in carbon isotopes from paleosols of the southern Chinese Loess Plateau. *Geology* 26, 987–990.
- Werger, M.J., Coetzee, B.J., 1978. The Sudano-Zambezian region. In: Werger, M.J. (Ed.), *Biogeography and Ecology of Southern Africa*. W. Junk, The Hague, pp. 301–462.
- Western, D., van Praet, C., 1973. Cyclical changes in the habitat and climate of an East African ecosystem. *Nature* 241, 104–106.
- Wolpoff, M.H., 1980. *Paleoanthropology*. Alfred A. Knopf, Inc., New York.
- Wynn, J.G., 2000. Paleosols, stable carbon isotopes, and paleoenvironmental interpretation of Kanapoi, Northern Kenya. *J. Hum. Evol.* 39, 411–432, doi:10.1006/jhev.2000.0431.